THE ANALYSIS AND TESTING OF THE QUAIFE TORQUE-BIASING DIFFERENTIAL

by

JOHN W. H. TROUT

Presented to the Faculty of the Graduate School of

The University of Texas at Arlington in Partial Fulfillment

of the Requirements

for the Degree of

MASTER OF SCIENCE IN MECHANICAL ENGINEERING

THE UNIVERSITY OF TEXAS AT ARLINGTON

MAY 2011

ACKNOWLEDGEMENTS

Special Thanks go to Dr. Robert Woods and the University of Texas in Arlington Formula Society of Automotive Engineers team for allowing me to use one of their Formula SAE racecars for the purpose of my testing. Special Thanks also go to Scotty at Taylor Race Engineering for teaching me how to rebuild the Quaife differential, for differential parts, and for help in understanding the Quaife differential.

April 4, 2011

ABSTRACT

THE ANALYSIS AND TESTING OF THE QUAIFE TORQUE BIASING DIFFERENTIAL

John Trout, M.S.

The University of Texas at Arlington, 2011

Supervising Professor: Robert L. Woods, Ph. D.

The purpose of this thesis is to analyze and test the Quaife torque biasing differential. The differential was modeled mathematically and equations were formulated. Experiments were then performed on a Formula SAE car to see how the output torque of each axle would react to modified preload torques. The results of these tests were then compared with the mathematical models. Overall, it was found that the there are two equations that govern the differential: one for traction and one for slip, and that the derived model correlates well with the experimental results.

TABLE OF CONTENTS

LIST OF ILLUSTRATIONS

Figure Page

LIST OF TABLES

CHAPTER 1

INTRODUCTION

This paper is an investigation into the torque biasing characteristics of the Quaife differential. The bias ratio of a differential is the ratio of output torque to the input torque of the differential. This research paper will answer the following questions: What is the mathematics that describes the Quaife differentials operation, and how does the preload torque affect the bias ratio in the differential?

The purpose of a differential on a vehicle is to allow the tires to rotate at different speeds when traveling through a corner. Without this differentiation the tires would experience equal torque and in order to turn, one tire would need to break traction against the road surface.

There are five types of differentials: spool, open, locked, limited-slip, torque-sensing. The spool replaces the differential and splits the torque equally at all times. In order for a vehicle to turn with a spool, the inside tire must break traction. An open differential requires that the torque of the drive train is equal on both tires. This type is ideal for allowing the vehicle to turn, but when one tire breaks traction neither tires has torque. The locked differential acts similarly to an open differential in that it allows equal distribution of torque between the tires when both tires have traction. When one tire loses traction a locking mechanism engages within the differential and splits the torque 50/50 like a spool. This prevents the tire with the least amount of traction from spinning, and allows the tire with the most traction to continue rotation. The limited-slip differential constantly splits the torque to allow the tires to rotate at different speeds during a turn, but does not allow any one tire 100% of the torque in any traction condition. When one tire loses traction, the clutch type limited-slip differentials use the friction of the clutches rotating against each other prevent that tire from spinning. This prevention sends

the available torque to the tire with the most traction. A problem with the clutch type limited-slip differential is that over time the clutches will lose effectiveness and the differential will behave like an open differential. The torque-sensing differentials use gears to constantly bias torque between the tires. The bias ratio in the differential determines the amount of torque sent to the tire with the most amount of traction in a slip condition or during a turn. The bias ratio is determined by the internal gear configurations and prevents tire spin by the gear forces within the differential casing. The torque-sensing differential is advantageous because it exhibits characteristics of both the open differential and the limited-slip differential: it allows the tires to rotate at different speeds during a turn, but during a low traction condition it sends torque to the tire with the most traction. This type of differential is the best since it has a simple design, and it has no friction surfaces that can wear out (Quaife Differential, 2011). Two makes of the gear type limited-slip differential are the Torsen and the Quaife. The operation of the Torsen differential has been extensively studied in 1988 (Chocholek, 1988). The purpose of this thesis is to mathematically model and test the Quaife differential. This thesis will analyze the operation of the Quaife limited-slip differential, develop equations that describe the model of the differential, test the differential, and compare the test data with the model.

CHAPTER 2

ANALYSIS

2.1 Components

The Quaife differential is comprised of the following five major components: the case, the sun gears, the planetary gears, the end plates, and the spring pack. The components of the spring pack consist of six Bellville washers, the star idler, and the two star idler cups. These components are modeled in Figure 1.

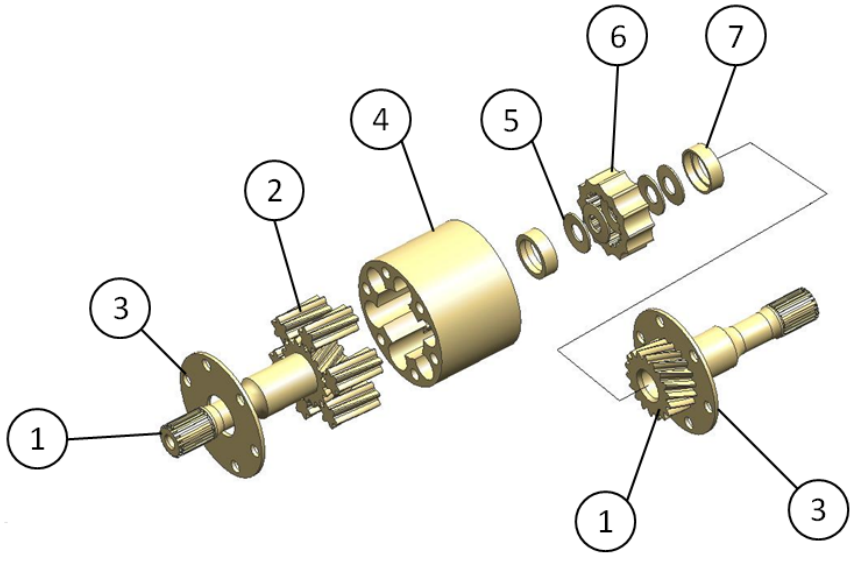

Figure 2.1: Exploded Model of the Quaife Differential

1. Sun Gear
2. Planetary Gear Set
3. End Plate
4. Case
5. Bellville Washers
6. Star Idler
7. Star Idler Cups

The case is a steel or aluminum shell that transmits the applied torque to the planetary gears. It houses the sun gears, the planetary gears, and the spring pack. It has six bolt holes on each side that are used by the end plates and sprocket or brake rotor for attachment. When the end plates are bolted onto the case ends, they press the sun gears against the spring pack and contain the movement of the planetary gears. The case can be seen below:

Figure 2.2: Quaife Differential Case

There are two sun gears that provide an output torque from the differential to the tires by means of the axles of the vehicle. These have a helical gear tooth pattern and are symmetrical to each other. The interface between the sun gears occurs through a set of six helical planetary gears per sun gear. It can be seen in Figure 3 that the planetary gears are aligned axially to the side gears.

Figure 2.3: Axial Alignment of Planetary Gears to Sun Gears

The spring pack, shown in Figure 4, lies in the center section of the case between the two sun gears. The components of the spring pack include a star shaped idler, two externally splined cups that fit into the star idler, and six Bellville spring washers. The star shaped idler holds the two externally splined cups. In these cups the washers are positioned to apply an axial load. Since the cups are splined to the star ring, it can be seen that the washers are not allowed to rotate or slide on each other.

Figure 2.4: Spring Pack Assembled

The stiffness of the spring pack rests in the orientation of the six Bellville washers and is directly proportional to the amount of torque required to break the internal friction of the differential. The position of the Bellville washers from the factory is modeled below, where from left to right it alternates cup-to-cone three times:

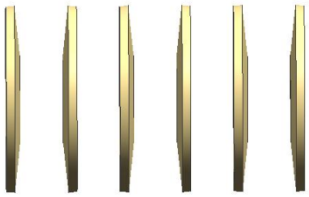

Figure 2.5: Configuration of the Factory Spring Pack Bellville Washers

The assembled model of the differential including a sprocket and brake rotor can be seen below:

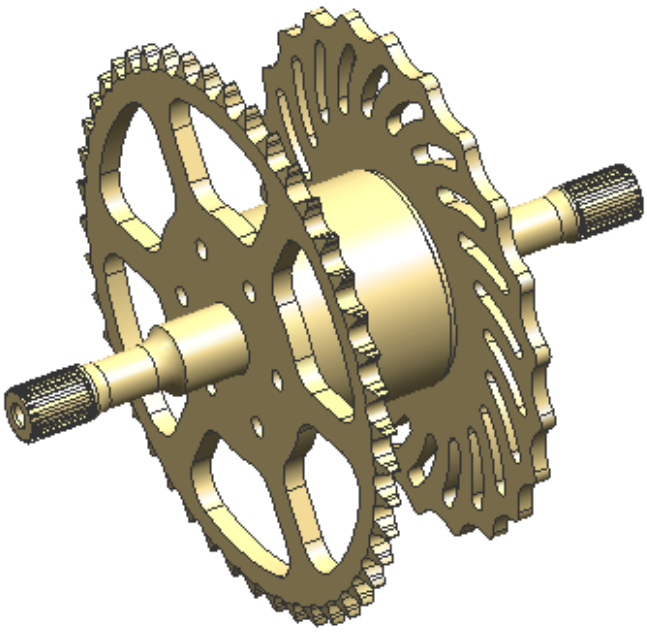

Figure 2.6: Assembled Model of the Quaife Differential

2.2 Model

The torque bias between the output shafts of the Quaife differential is governed by several key design parameters including the pitch radius of the sun gears and planetary gears, the associated helix and pressure angles, the radius of the array of the planetary gears, and the coefficient of friction between all of the components. When a drive torque is applied on the sprocket it transfers to the planetary gears and into the case. This is shown below:

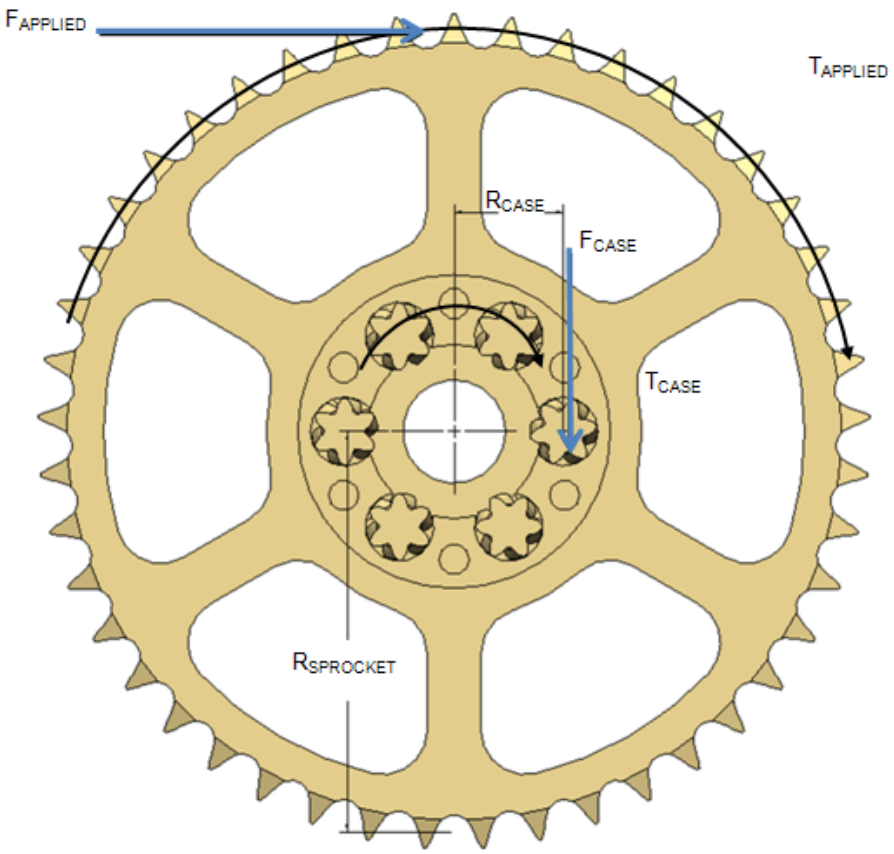

Figure 2.7: Transmission of Torque from the Sprocket to the Planetary Gears

Where:

$R_{SPROCKET}$ = Sprocket Radius

R_{CASE} = Radius to Planetary Gear

F_{CASE} = Force that Planetary Gear Applies to Case Pocket

$F_{APPLIED}$ = Applied Drive Force

T_{CASE} = Planetary Gear Torque Applied to Case

$T_{APPLIED}$ = Applied Drive Torque

The applied drive torque, $T_{APPLIED}$, is equal to the torque applied to the differential case, T_{CASE}. The equation for the force applied to the planetary gears from the differential casing, F_{CASE}, is shown below:

$$F_{CASE}R_{CASE} = F_{APPLIED}R_{SPROCKET}$$

$$F_{CASE} = \frac{F_{APPLIED}R_{SPROCKET}}{R_{CASE}} \quad (1)$$

As the case rotates forward due to the applied torque and the tires of the vehicle are rotating at different speeds during a turn, the case applies a normal force to the planetary gears as they rotate.

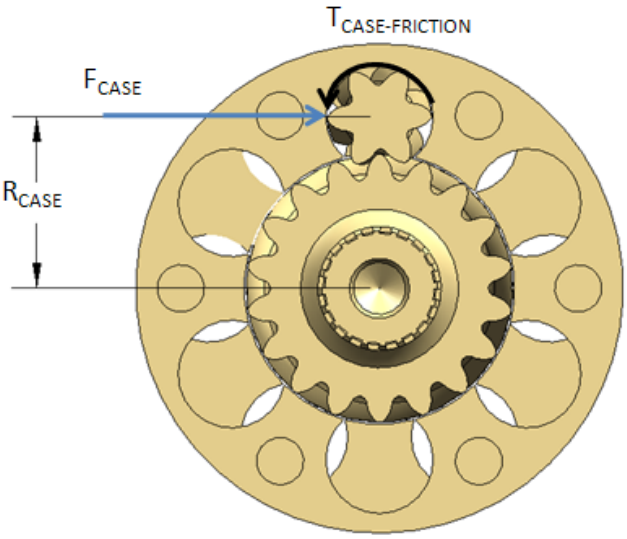

Figure 2.8: Friction between the Differential Case and the Planetary Gears

The point at which the differential breaks loose is when the applied forces are greater than or equal to the force required to break the static friction. This can be seen in Figure 9.

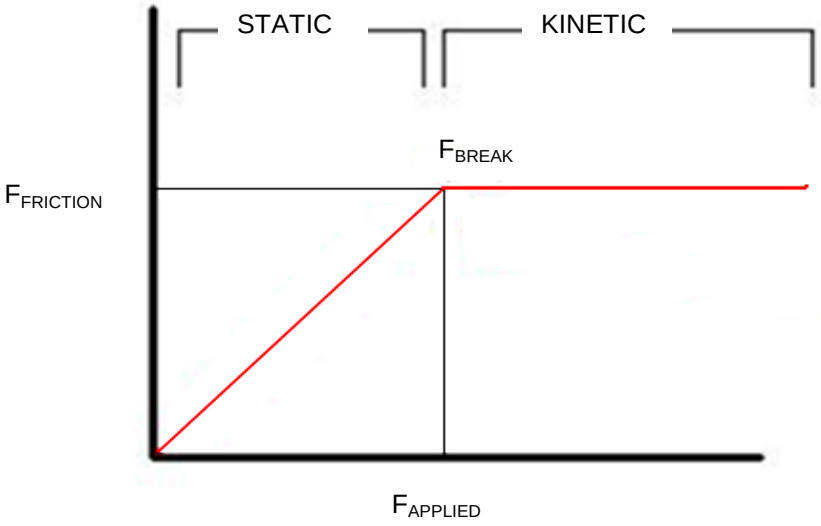

Figure 2.9: Break Force of Static to Kinetic Friction
Static & Kinetic Friction (2011, March 21)

The break friction is the point at which the differential begins to differentiate and is when the static friction transitions to kinetic friction. The equation for the break friction is:

$$F_{BREAK} = F_{NORMAL}\mu = F_{CASE}\mu$$

Where μ is the kinetic coefficient of friction.

Since $F_{FRICTION}$ is a function of $F_{APPLIED}$, the following two rules apply for this graph:

1. If $F_{APPLIED} < F_{BREAK}$, then $F_{FRICTION} = F_{APPLIED}$
2. If $F_{APPLIED} \geq F_{BREAK}$, then $F_{FRICTION} = F_{BREAK}$

The torque required to overcome the break friction between the case and the planetary gears is then found using the following equation:

$$T_{CASE-FRICTION} = F_{BREAK}R_{CASE}$$

$$T_{CASE-FRICTION} = F_{CASE}R_{CASE}\mu = T_{CASE}\mu \qquad (2)$$

As the differential applies forward torque it sends the planetary and sun gears outward against the end plates. This transmission is illustrated in Figure 2.10.

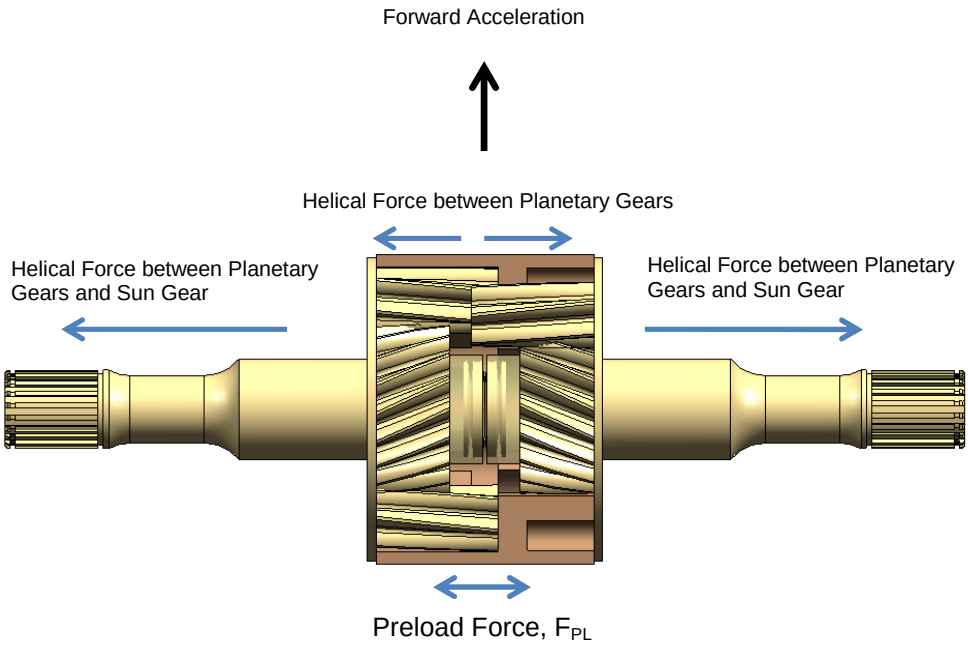

Figure 2.10: Outward Motion of Internals during Forward Acceleration

When one tire begins to rotate at a slower rate than the other tire, such as when a vehicle is making a turn, the slower side sends its planetary gears towards the traction side from the influence of the helix angles. For the case of a left hand turn, this is illustrated in Figure 11.

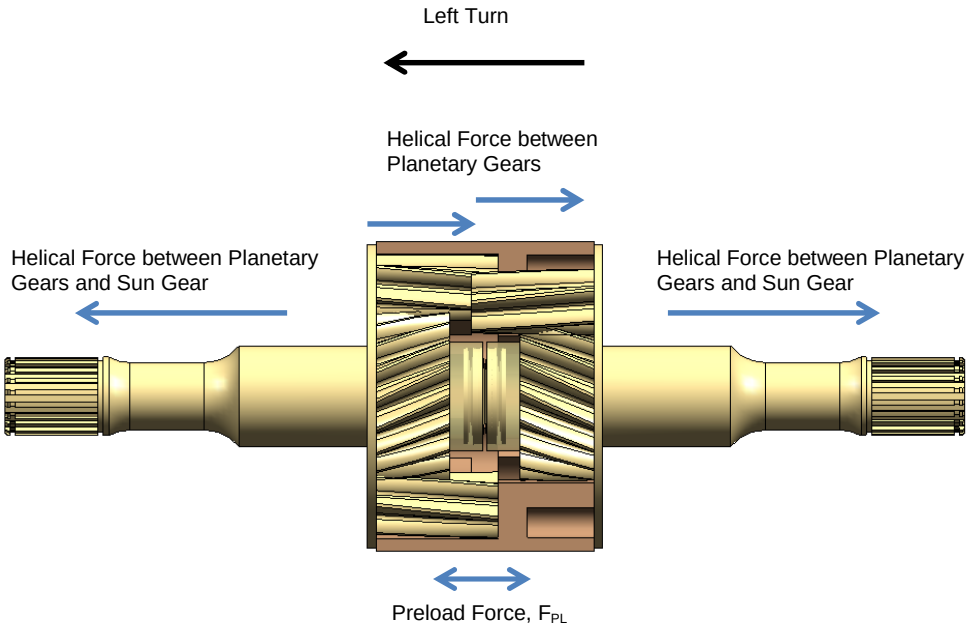

Figure 2.11: When Turning Left Internals Move Right

In this case the friction that must be overcome in order for the differential to perform includes the friction between case and the planetary gears, the sun gears and their end plates, the left set of planetary gears and the internal shelves of the case, plus the right set of planetary gears and the right end plate. The friction between the meshing of gears has been extensively studied in previous texts; in this case this friction is negligible.

As the case rotates it sends a force normal to the axis of rotation to the planetary gear. The helix and pressure angles force the left set of planetary gears against the internal shelves of the casing and the right set of planetary gears against the end plate. The resistance for the planetary gears to rotate comes from the coefficient of friction between the end plate or case and the planetary gear. The torque required to break the friction against the end plate is equal to the torque required to break the friction against the internal shelves of the case. A model of the planetary gear interfacing with the end plate is shown in Figure 12.

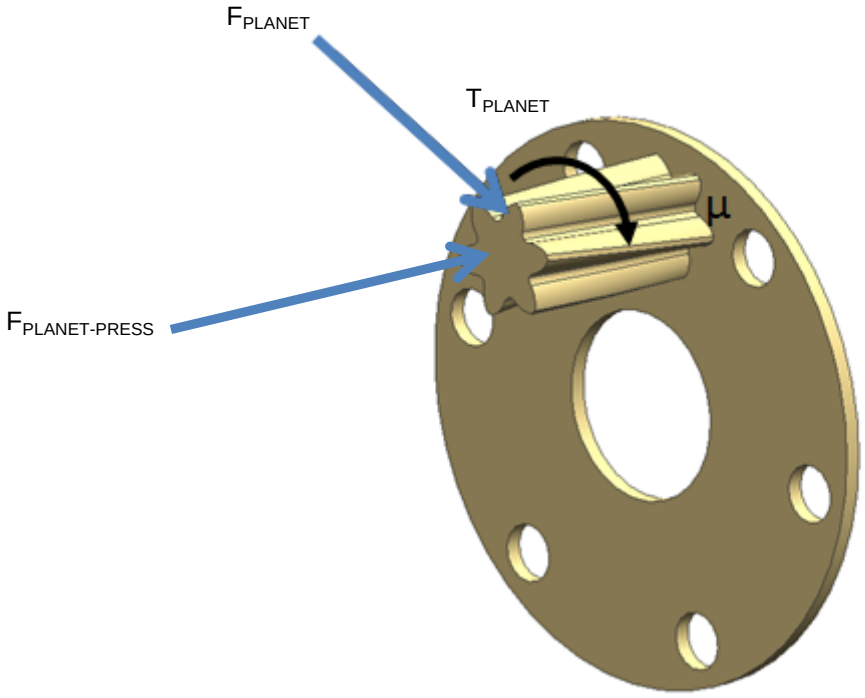

Figure 2.12: Planetary Gear Forced Against End Plate

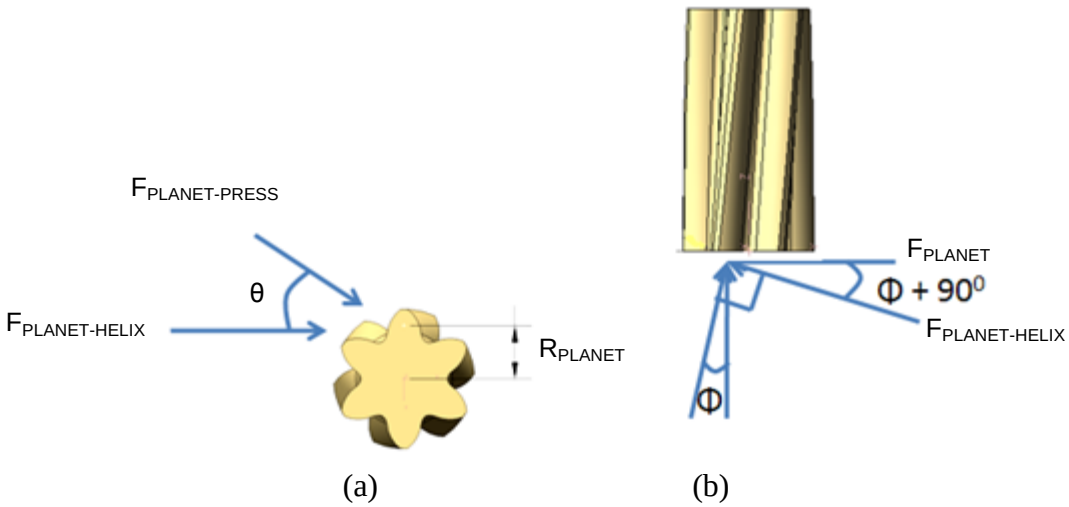

Figure 2.13: Planetary Gear's (a) Pressure Angle and (b) Helix Angle

Where:

$T_{PLANET\text{-}FRICTION}$ = Torque to Break Planetary Friction

T_{PLANET} = Planetary Gear Torque

F_{PLANET} = Planetary Gear Force

$F_{PLANET\text{-}HELIX}$ = Planetary Gear Helix Angle Force

$F_{PLANET\text{-}PRESS}$ = Planetary Gear Pressure Angle Force

R_{PLANET} = Planetary Pitch Radius

R_{CASE} = Case Radius

Φ = Helix Angle

θ = Pitch Angle

μ = Coefficient of Friction

From Figures 13(a) and 13(b), it can be seen how the planetary gear force translates into a force that pushes the planetary gears into the end plate. This force, $F_{PLANET\text{-}PRESS}$ is found using the equations below, where $T_{APPLIED}$ is equal to T_{PLANET} (Mott, 2004):

$$T_{APPLIED} = F_{PLANET}(R_{PLANET} + R_{CASE})$$

$$F_{PLANET} = \frac{T_{APPLIED}}{(R_{PLANET} + R_{CASE})} \quad (3)$$

$$F_{PLANET-HELIX} = F_{PLANET} \sin(90^{o} + \varphi) = F_{PLANET} \cos\varphi$$

$$F_{PLANET-PRESS} = F_{PLANET-HELIX} \cos\theta$$

The torque required to break the planetary friction is found using the following equations (Mott, 2004):

$$T_{PLANET-FRICTION} = F_{PLANET-PRESS} R_{PLANET} \mu$$

$$T_{PLANET-FRICTION} = \frac{T_{APPLIED} R_{PLANET} \mu}{(R_{PLANET} + R_{CASE})} \cos\varphi \cos\theta \qquad (4)$$

The next torque that needs to be found is the torque required to overcome the friction between the sun gear and the end plate. As the internal gearing differentiates, the meshing of the planetary gears to the sun gear forces the sun gear into the end plate. The resistance for the sun gear to rotate comes from the coefficient of friction between the end plate and the sun gear. This is illustrated in Figure 14.

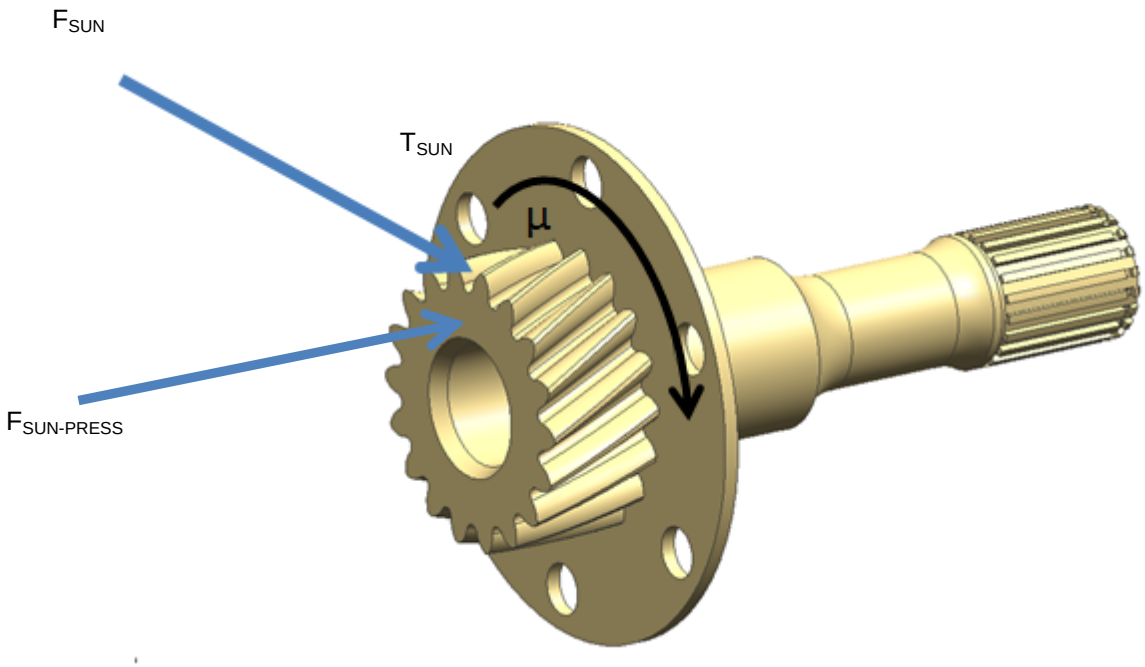

Figure 2.14: Sun Gear Forced Against End Plate

The force that pushes the sun gear into the end plate, $F_{SUN-PRESS}$, is found below (Mott, 2004):

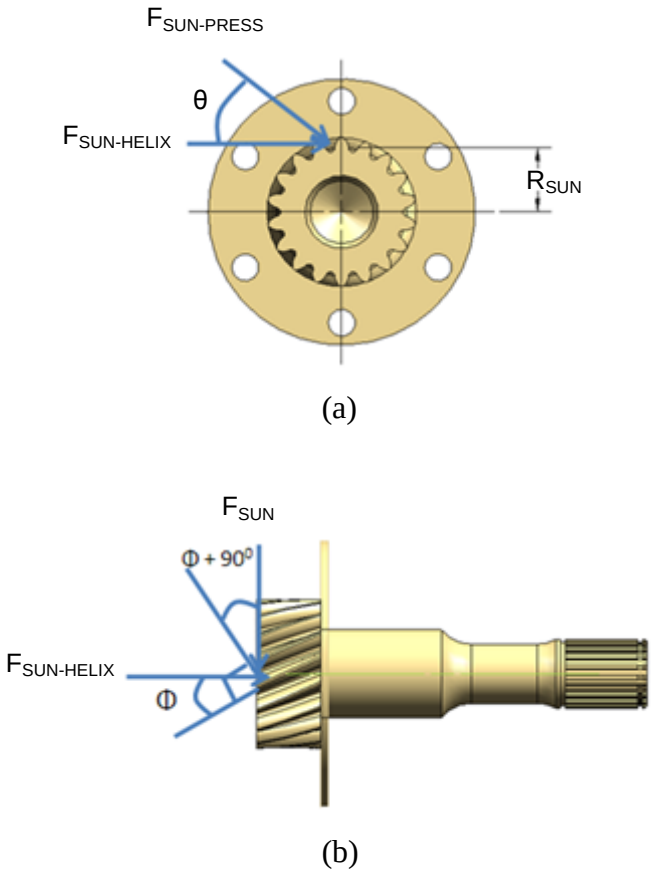

Figure 2.15: Sun Gear's (a) Pressure Angle and (b) Helix Angle

Where:

$T_{SUN-FRICTION}$ = Torque to Break Sun Friction

T_{SUN} = Sun Gear Torque

F_{SUN} = Sun Gear Force

$F_{SUN-HELIX}$ = Sun Gear Helix Angle Force

$F_{SUN-PRESS}$ = Sun Gear Pressure Angle Force

Φ = Helix Angle

θ = Pitch Angle

μ = Coefficient of Friction

R_{CASE} = Case Radius

R_{SUN} = Sun Gear Pitch Radius

From Figures 2.14 and 2.15 it can be seen how the sun gear force translates into a force that pushes the sun gear into the end plate. This force, $F_{SUN\text{-}PRESS}$ is found using the equations below, where $T_{APPLIED}$ is equal to T_{SUN} (Mott, 2004).

$$T_{APPLIED} = F_{SUN} R_{SUN}$$

$$F_{SUN} = \frac{T_{APPLIED}}{R_{SUN}}$$

$$F_{SUN-HELIX} = F_{SUN} \sin(90^{O} + \varphi) = F_{SUN} \cos\varphi$$

$$F_{SUN-PRESS} = F_{SUN-HELIX} \cos\theta$$

The torque required to break the planetary friction is found using the following equations (Mott, 2004):

$$T_{SUN-FRICTION} = F_{SUN-PRESS} R_{SUN} \mu$$

$$T_{SUN-FRICTION} = \frac{T_{APPLIED} R_{SUN} \mu}{R_{SUN}} \cos\varphi\cos\theta$$

$$T_{SUN-FRICTION} = T_{APPLIED} \mu\cos\varphi\cos\theta \qquad (5)$$

2.3 Governing Equations

The governing equations for the Quaife differential are of the form:

$$T_{TRACTION} = T_{TOTAL} + T_{PRELOAD}$$

$$T_{SLIP} = T_{APPLIED} - T_{TOTAL} - T_{PRELOAD}$$

The equation for T_{TOTAL} is found by taking a sum of the torques required to break the static friction of the internal components of the differential. This equation is:

$$T_{TOTAL} = T_{CASE\text{-}FRICTION} + 2T_{PLANET\text{-}FRICTION} + 2T_{SUN\text{-}FRICTION}$$

The torque $T_{PLANET\text{-}FRICTION}$ is multiplied by two because during differentiation there are two sets of planetary gears overcoming friction, one against the casing and one against the end plate. The torque $T_{SUN\text{-}FRICTION}$ is multiplied by two because during differentiation both sun gears are pressed against their respective end plates by the preload spring pack. The total torque for the Quaife differential is:

$$T_{TOTAL} = T_{APPLIED}\mu + 2\frac{T_{APPLIED}R_{PLANET}\mu}{(R_{PLANET} + R_{CASE})}\cos\varphi\cos\theta + 2T_{APPLIED}\mu\cos\varphi\cos\theta$$

After normalizing, the equation is:

$$T_{TOTAL} = T_{APPLIED}\mu\left[1 + 2\frac{R_{PLANET}}{(R_{PLANET} + R_{CASE})}\cos\varphi\cos\theta + 2\cos\varphi\cos\theta\right]$$

This equation can be rewritten as:

$$T_{TOTAL} = T_{APPLIED} f_L$$

Where f_L is the loaded frictional torque that is equal to the product of coefficient of friction with the equation in the brackets. The final equations for the Quaife differential are:

$$T_{TRACTION} = T_{APPLIED} f_L + T_{PRELOAD} \quad (6)$$

$$T_{SLIP} = T_{APPLIED} - T_{APPLIED} f_L - T_{PRELOAD} \quad (7)$$

The bias ratio can then be found using the following equation:

$$\text{BIAS RATIO} = \frac{T_{TRACTION}}{T_{APPLIED}} \quad (8)$$

The bias ratio determines the amount of torque that is sent to the tire with the most amount of traction. This ratio needs to be high, but not to equal one where the differential no longer biases torque and does not allow differentiation. The equations in this section model the operation of the Quaife differential. They show how the radii, the helix angles, and the pressure angles of the components interact with each other to bias torque. It can be seen from these equations that the variables that are the most influential in the system are the preload torque and the coefficient of friction. It can also be seen that there are two equations that govern the Quaife differential: the traction equation and the slip equation.

2.4 Model Simulation

This section simulates the Quaife differential using the Equations (6) and (7) that were derived for traction and slip. The preload torque and the coefficient of friction are the two variables that were simulated. The first simulation shows how the preload affects the output torque of the differential, when the coefficient of friction is constant.

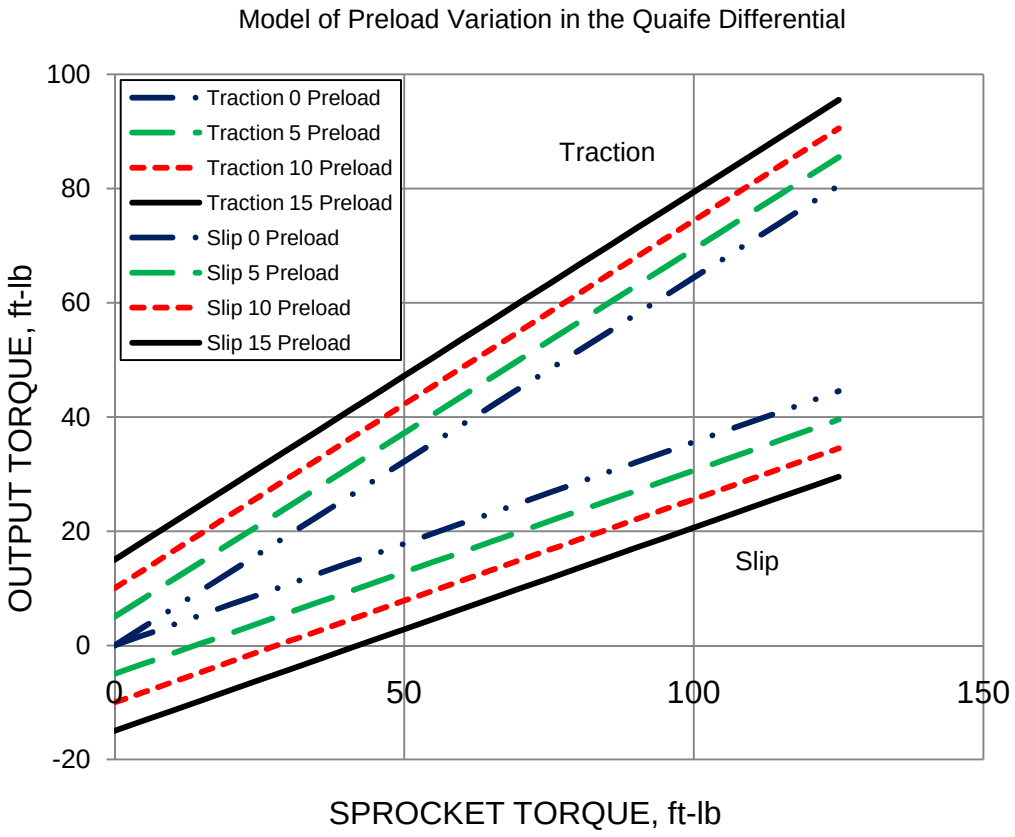

Figure 2.16: Plots of Traction and Slip Models

It can be seen that by the varying the preload of the spring pack the slope of the curves remain the same, while the initial point on the output torque axis moves up or down depending on the preload. The bias ratios for this simulation can be seen in Table 2.1.

Table 2.1: Bias Ratios for Modified Preload in Quaife Differential Model

	Applied	Traction	
Preload, (lb_f ft)	**Torque (lb_f ft)**		**BIAS RATIO, %**
0	125	80.50	64.40
5	125	85.50	68.40
10	125	90.50	72.40
15	125	95.50	76.40

It can be seen that the bias ratio increases as the preload increases. The second simulation varied the coefficient of friction from 0 to 0.4 while the preload was set to zero. This can be seen in Figure 2.17.

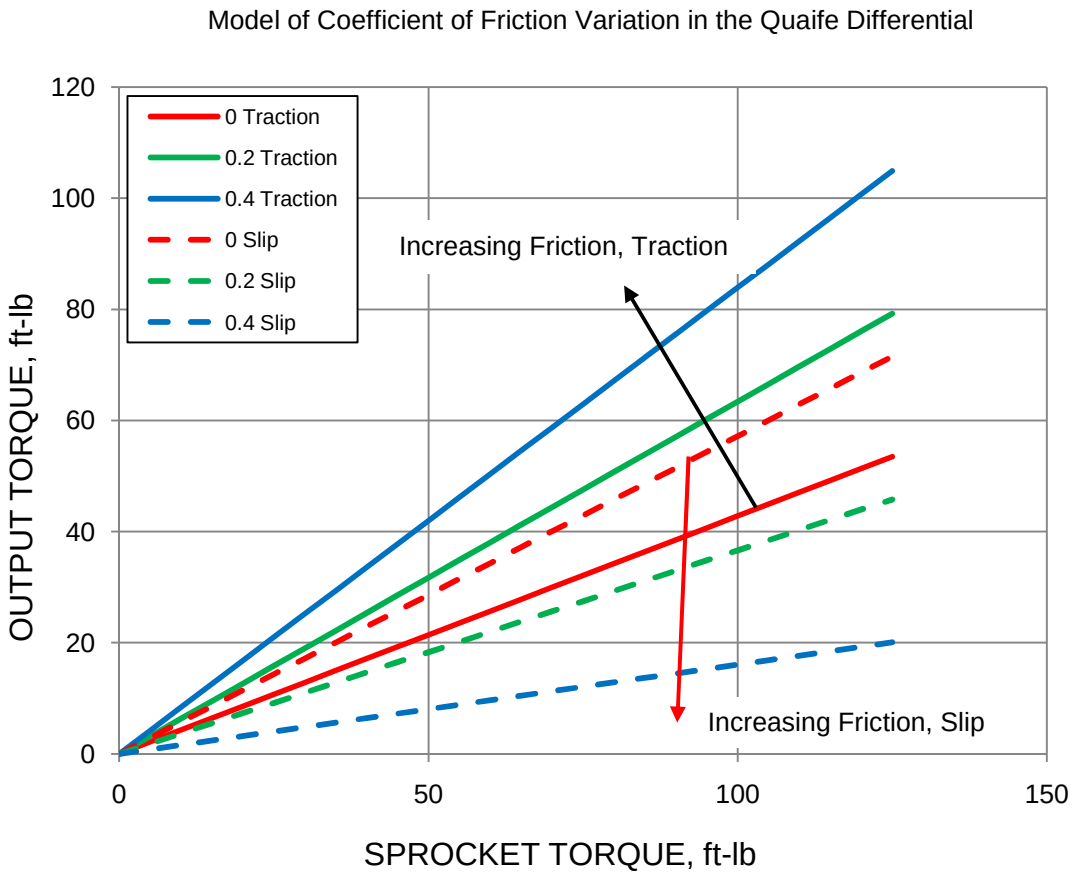

Figure 2.17: Effect of Higher Friction in the Quaife Differential

It can be seen that increasing the coefficient of friction increases the traction slope and decreases the slip slope. When the traction slope becomes steeper to the point that the biasing ratio becomes 100% the differential locks ups and no longer biases torque. The bias ratios for this simulation are shown in Table 2.2.

Table 2.2: Bias Ratios for Modified Coefficient of Friction in Quaife Differential Model

	Applied	**Traction**	
Coefficient of Friction	**Torque (lb_f ft)**		**BIAS RATIO, %**
0.00	125.00	53.50	42.80
0.20	125.00	79.21	63.37
0.40	125.00	104.91	83.93

To attain a high coefficient of friction, dissimilar materials or dry surfaces could be employed. Several high coefficient of friction combinations can be seen in Table 2.3.

Table 2.3: Known Coefficients of Friction for Various Material Combinations
Friction and Coefficients of Friction (2011, March 4)

Material Combinations		Coefficient of Friction - μ_s	
		Dry Surfaces	Lubricated Surfaces
Aluminum-bronze	Steel	0.45	
Aluminum	Mild Steel	0.61	
Brass	Steel	0.35	0.19
Bronze	Steel		0.16
Bronze - sintered	Steel		0.13
Cadmium	Mild Steel	0.46*	
Cast iron	Mild Steel	0.4, 0.23*	0.21, 0.133*
Carbon	Steel	0.14	0.11 - 0.14
Copper-Lead alloy	Steel	0.22	
Copper	Mild Steel	0.53, 0.36*	0.18*
Graphite	Steel	0.1	0.1
Nickel	Mild Steel	0.64*	0.178*
Phosphor-bronze	Steel	0.35	
Steel	Steel	0.8	0.16
Tungsten Carbide	Steel	0.4-0.6	0.1 - 0.2

* Kinetic Friction

CHAPTER 3

TESTING

3.1 Test Setup

One of the research questions is how does the preload torque affect the bias ratio of the Quaife differential?

The Quaife differential was tested to determine how the bias ratio would be affected by varying the preload in the spring pack. The tests on the Quaife differential were conducted between January 24, 2011 and February 22, 2011 with the help of Dr. Robert Woods and the Formula SAE team at the University of Texas at Arlington. The test was performed on the 2008 UTA Formula SAE race car. To gain access to the area to test, the rear end of the car was raised on stands, the wheels and any interfering body panels were removed. The setup of the car can be seen below in Figure 3.1.

Figure 3.1: The 2008 UTA FSAE Racecar is Ready to be Tested

To test the differential, three torques values were needed: the input and the two outputs. The input load was applied to the sprocket by a chain, while the outputs torques were measured using torque wrenches at the hubs. Special hub adapters were needed to allow the torque wrenches to be placed at the center of the hub.

Figure 3.2: Special Hub Adapters

A load was then applied to the sprocket of the differential by means of a load on the chain, while two torque wrenches on the hubs were used to lift the load. To relieve the hysteresis in the system, both torque wrenches rotated against the load to lift it, then both lowered it. With the load still suspended, the test was then ready to begin. While one torque wrench was held at a constant position, the other torque wrench reduced its resistance against the load, or was allowed to “slip”. This mimicked a turn or losing traction from one tire. When the differential began to rotate towards the induced load of the sprocket, both readings on the torque wrenches were taken by observation. This test was then repeated to allow the other torque wrench to slip against the load. This test can be seen in Figure 3.3 as it was performed.

Figure 3.3: The Actual Testing of the Quaife Differential

The tests were performed for three different loads to the sprocket, with the loads pulling the sprocket both forward and backward, for acceleration and braking respectively. The torque to the sprocket, T_X, was found using the following equation relating the pitch radius of the sprocket, R_X to the load, F_X:

$$T_X = F_X R_X \tag{9}$$

The sled that was attached to the chain weighed 126.3 pounds; this weight included the cables and the part of the chain that the sprocket needed to lift. The medium weight included the sled and the cylinder. This combination weighed 191.9 pounds. The third weight was the sled plus the steel block, which weighed in at 324.4 pounds. The weights that were used for this test can be seen in Figure 3.4.

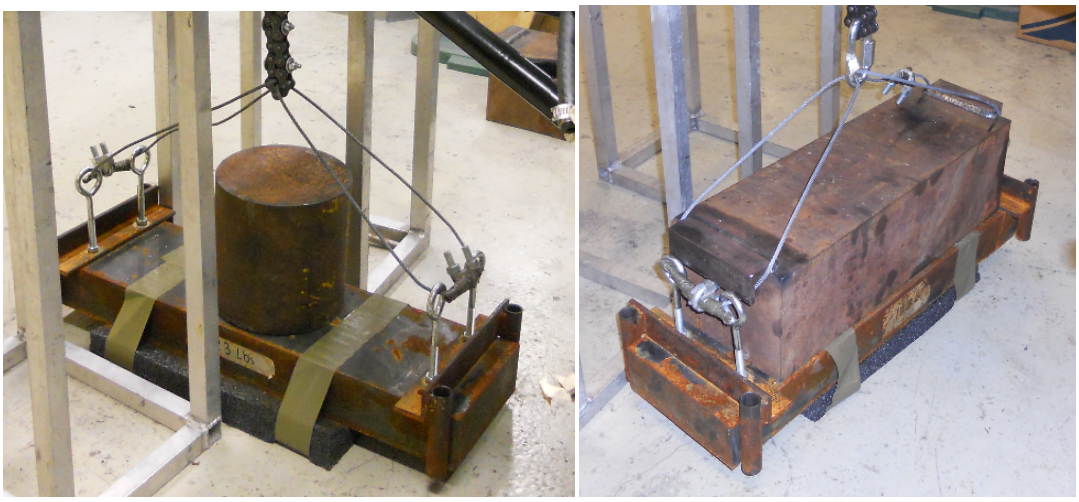

Figure 3.4: The Sled, the Cylinder, and the Steel Block Weights

The following table shows the input loads and corresponding torques to the sprocket using Equation (9):

Table 3.1: Conversion of Applied Loads to Torque

Applied Load, F_X (lb_f)	**Torque (lb_f ft)**
0.0	0.0
126.3	47.2
191.9	71.6
324.4	121.1

The preload was varied by removing Bellville washers, or adding shims. The shims were added between two cones of the Bellville spring washer stackup. An example of this stackup can be seen in Figure 3.5.

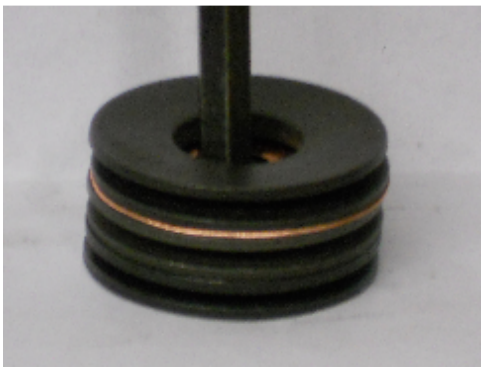

Figure 3.5: Factory Stackup Plus a Shim

3.2 Results

A total of six sets of data were recorded. These data sets include two stock configuration tests, one test with five washers, and three tests using the stock washer configuration plus three different thickness shims. The numerical results of these tests can be found in the Appendix section of this thesis. The following are plots taken from these results for the six tests.

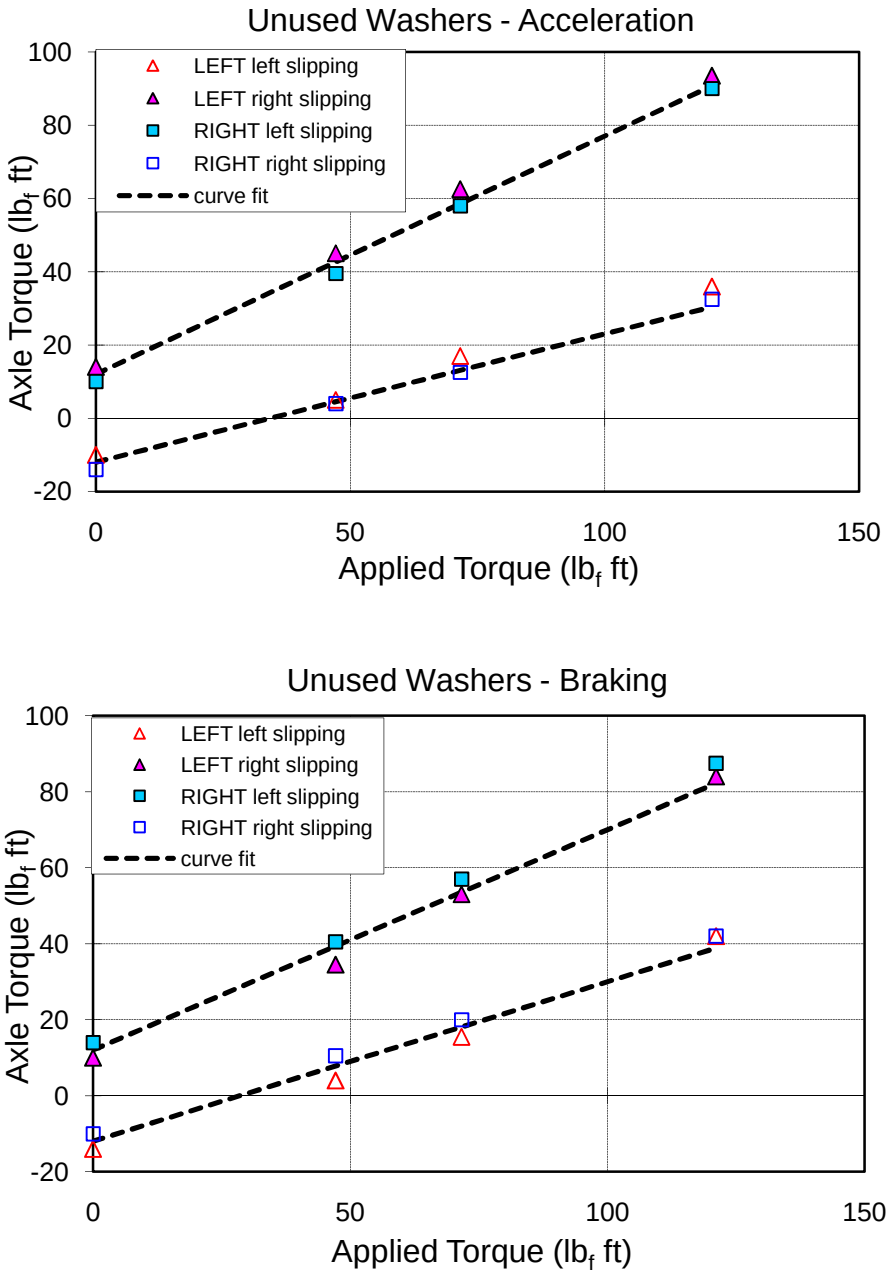

Figure 3.6: Stock Configuration using Unused Washers

The first experiment was conducted using the factory spring configuration and unused Bellville spring washers. The unused Bellville washers provided a preload torque of +/- 10 foot-pounds for acceleration and +/- 14 foot-pounds of torque for braking.

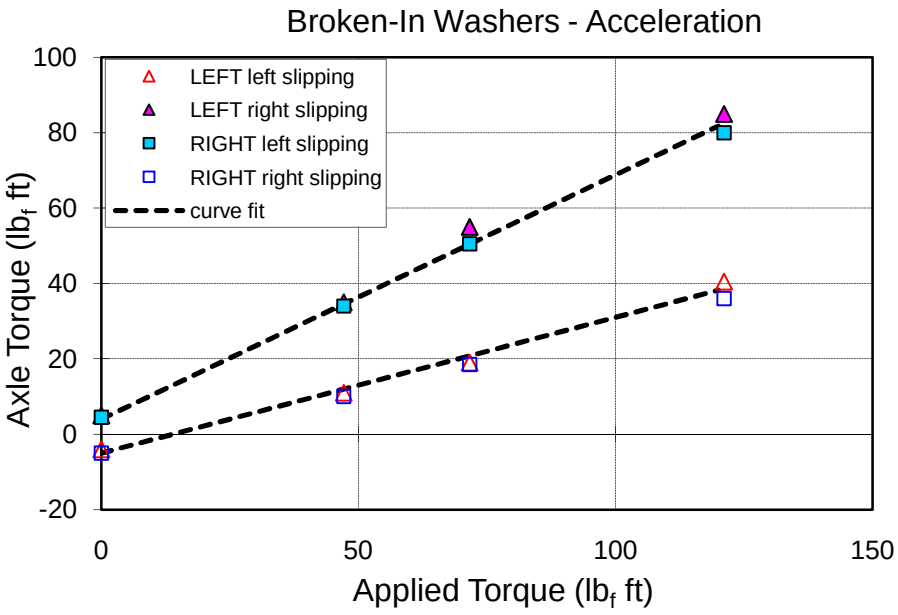

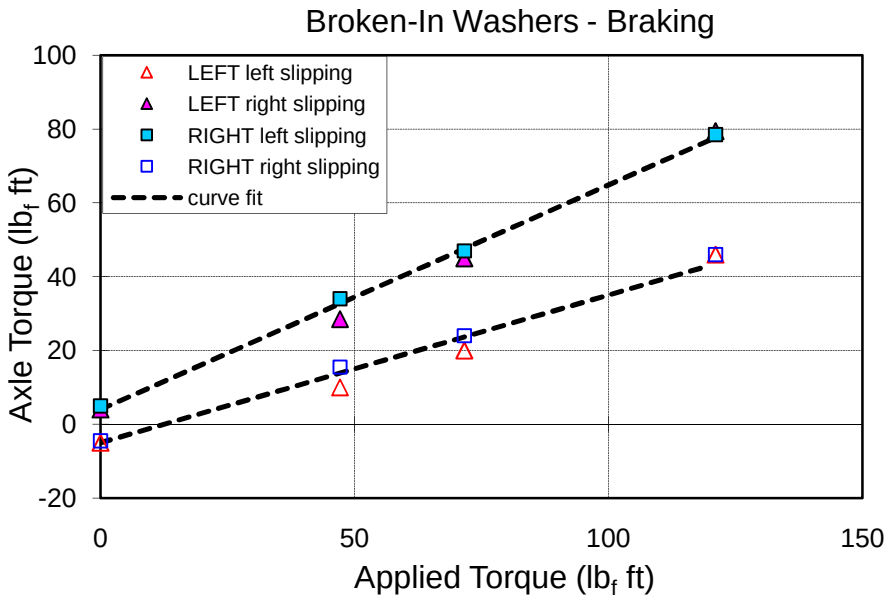

Figure 3.7: Stock Configuration using Broken-In Washers

This experiment was a repeat of the stock configuration after the Bellville washers were broken-in, by installing them in the differential ten times. The preload torque of the broken-in Bellville washers is +/- 4 foot-pounds for acceleration and +/- 5 foot-pounds of torque for braking.

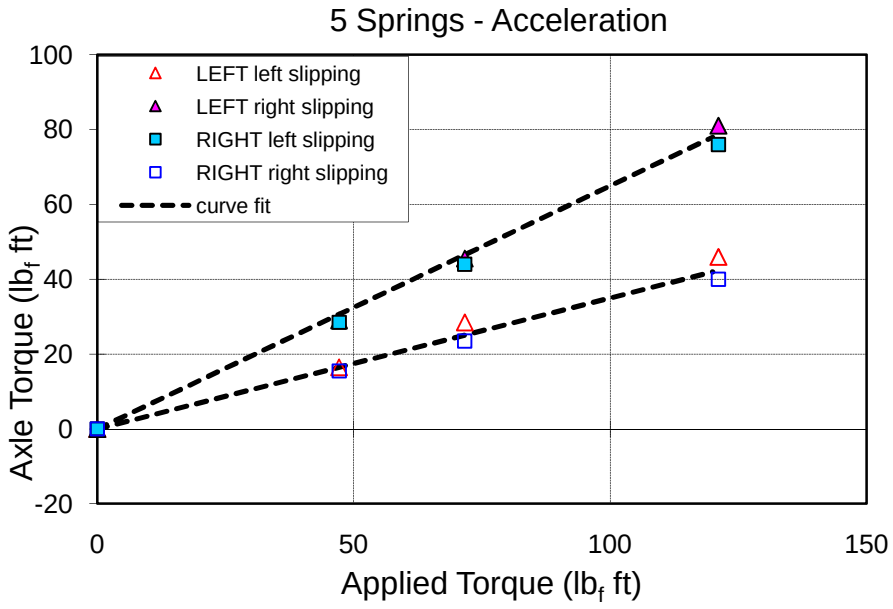

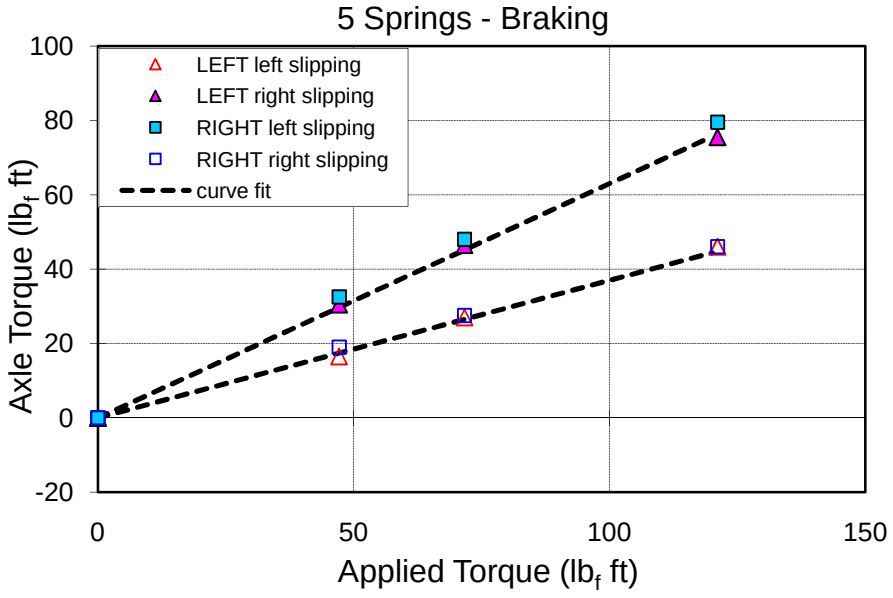

Figure 3.8: Configuration using Five Washers

This experiment only used five Bellville washers, which gave a zero preload value.

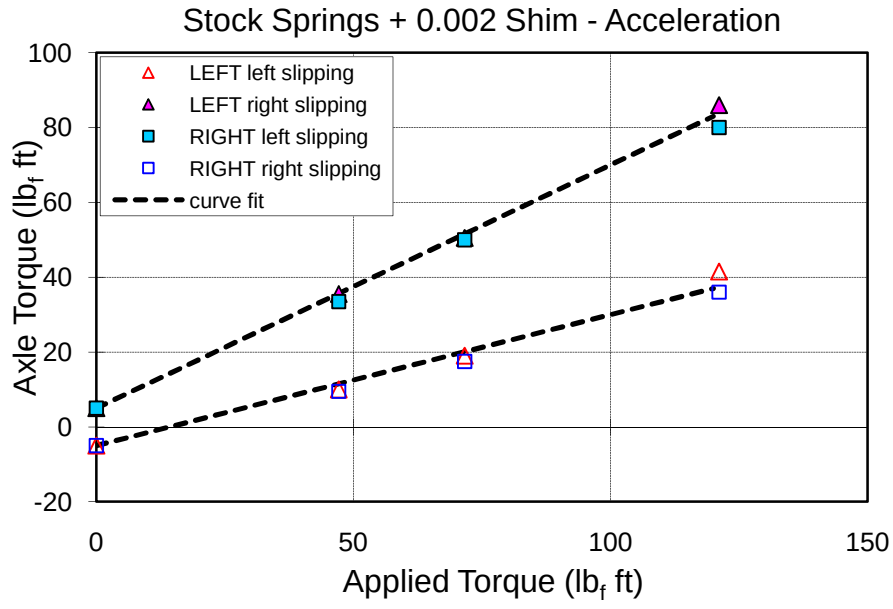

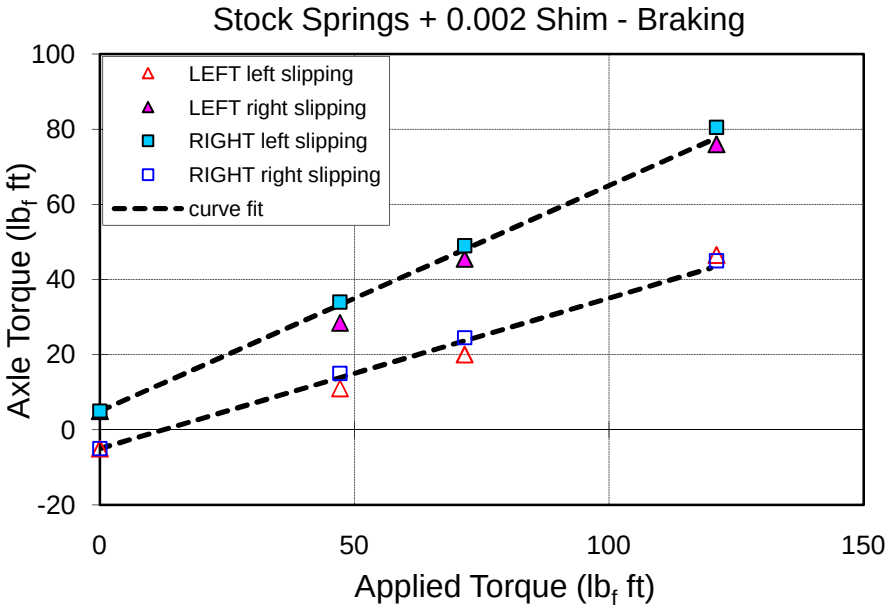

Figure 3.9: Stock Configuration Plus 0.002 Inch Shim

For the next experiment the differential was rebuilt using a 0.002 inch shim in the stackup. This yielded preload torque values of +/- 5 foot-pounds for both the acceleration and braking experiments.

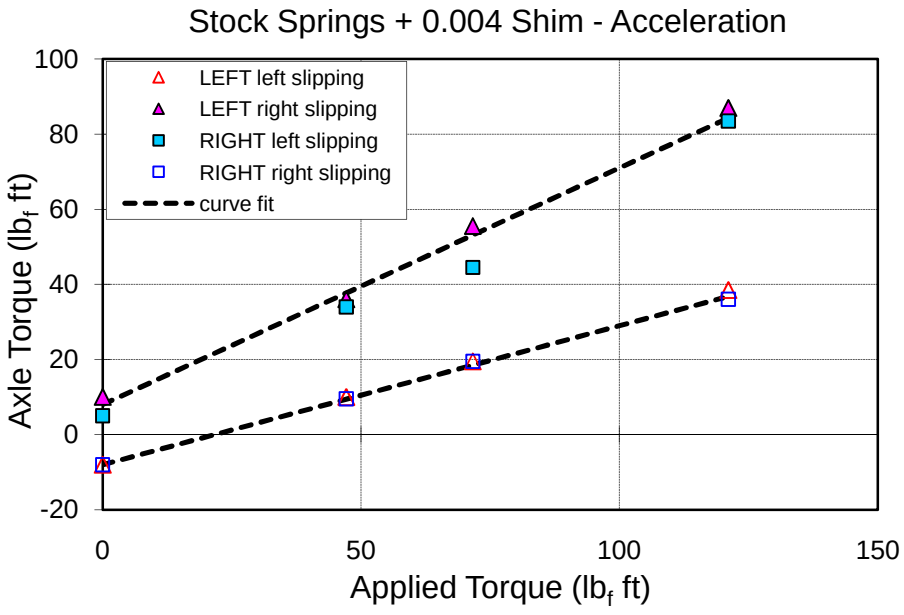

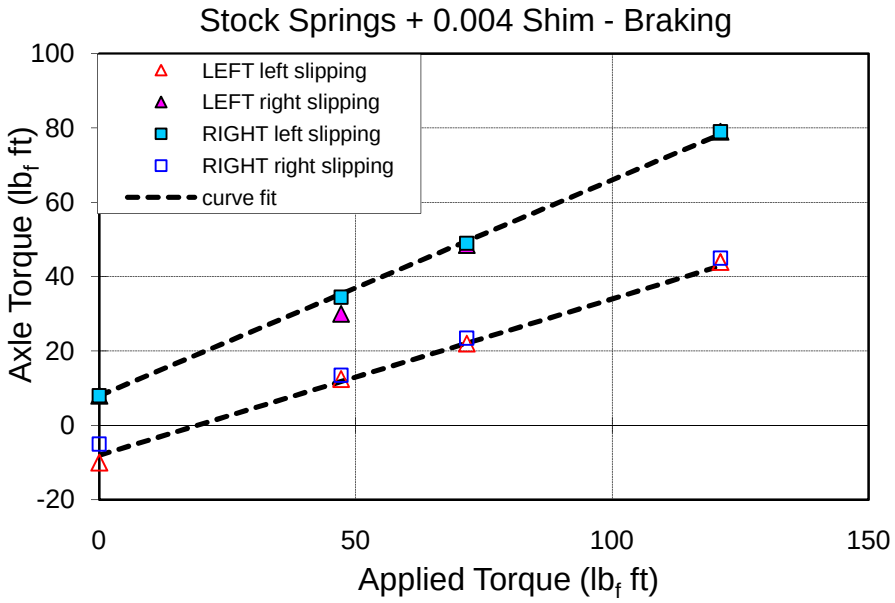

Figure 3.10: Stock Configuration Plus 0.004 Inch Shim

The differential was then rebuilt and the 0.002 inch shim was replaced with a 0.004 inch shim. Again, the preload torque value of +/- 8 foot-pounds is the same for both the acceleration and braking experiments.

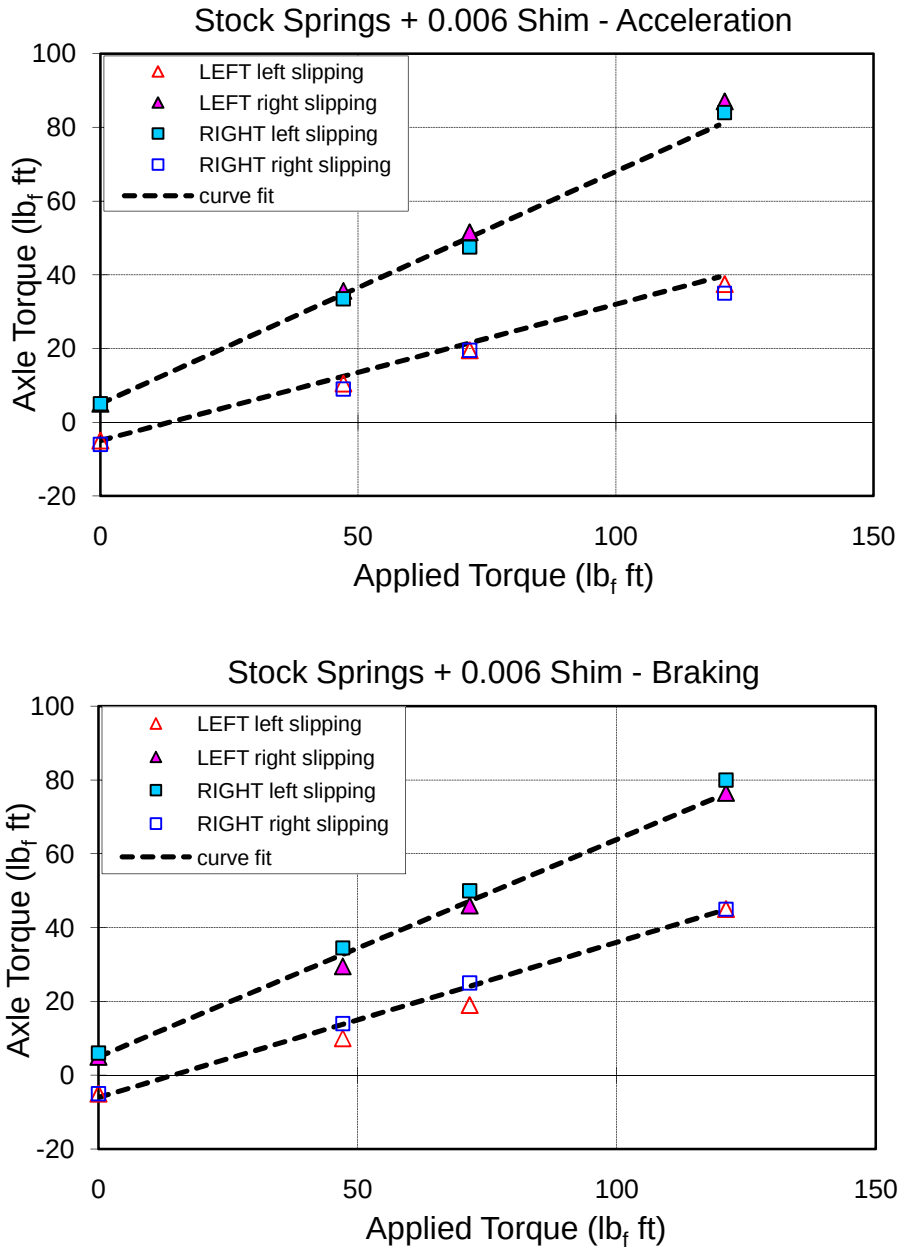

Figure 3.11: Stock Configuration Plus 0.006 Inch Shim

The last experiment was to replace the 0.004 inch shim with a 0.006 inch shim. This gave a preload torque of +/- 5 foot-pounds of torque for the acceleration experiment, and +/- 6 foot-pounds of torque for the braking experiment. It can be seen by all these results that the output

torque verses the sprocket torque was consistently linear for both the acceleration and braking experiments. It can also be seen that the slope on the upper part of all the graphs, which is the traction slope, is steeper than the lower slope on the graph, also called the slip slope. Table 3.2 summarizes the experimental data.

Table 3.2: Experimental Data Summary

	Acceleration			Braking		
Configuration	Preload, ft-lb	Slope Accel	Bias, %	Preload, ft-lb	Slope Braking	Bias,%
Unused	10	0.15	75	14	0.08	68
Broken-In	4	0.14	68	5	0.10	64
5 springs	0	0.15	65	0	0.13	63
0.002 Shim	5	0.15	69	5	0.10	64
0.004 Shim	8	0.13	70	8	0.08	65
0.006 Shim	5	0.13	67	6	0.08	63

Using the results shown in Table 3.2, the following graph shows how the preload affects the steepness of the traction slopes for the braking and acceleration tests.

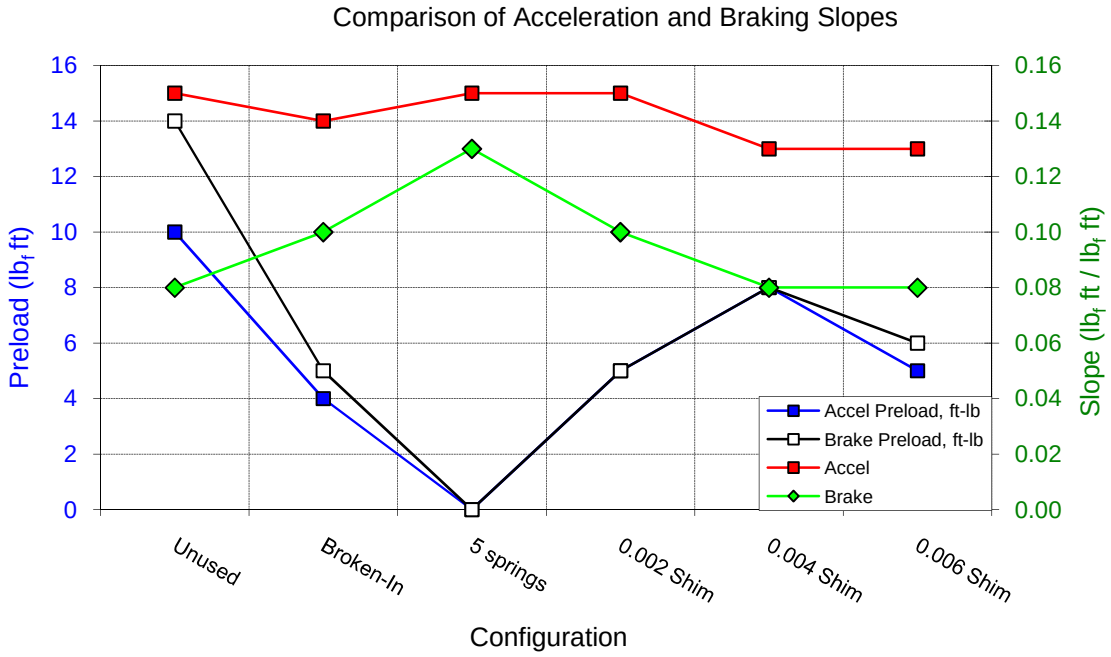

Figure 3.12: Effect of Preload on the Acceleration and Braking Slopes

It can be seen that the acceleration and braking preload curves follow the same trends. The slope of the acceleration ranges from 0.13 to 0.15, and 0.08 to 0.13 for braking. When the five washer configuration is employed the slopes of acceleration and braking are the most alike. If unused washers are tested, the acceleration and braking curves are least alike. Figure 3.13 is a graph that shows how the bias ratio changes for the six configurations.

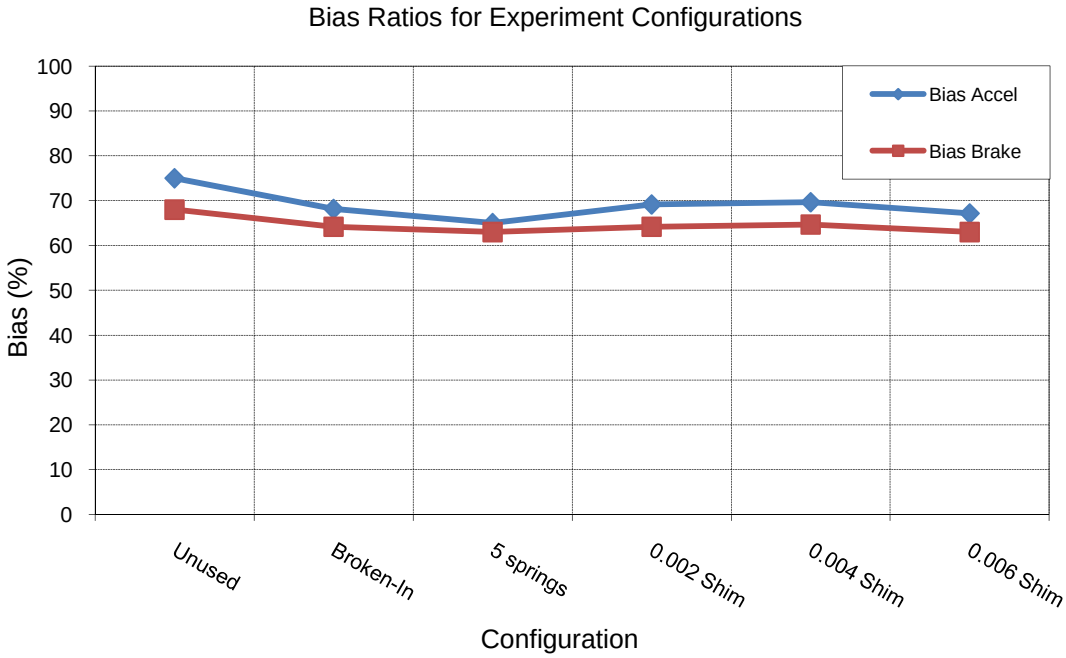

Figure 3.13: Changes in the Bias Ratio for the Different Configurations

It can be seen that the unused washers have the highest biasing ratio, while the configuration using only five washers has the lowest biasing ratio. The broken-in washer, the 0.002 inch shim and 0.004 inch shim configurations have a bias ratio of almost 70%. It is shown that the bias ratio increases from the five washer configuration to the configuration that adds the 0.004 inch shim, then begins to decrease. From these results it can be seen that the configuration using the unused Bellville washers is the best since it has the highest biasing ratio.

3.3 Comparison to Model

The results of the tests are then compared to plots derived from the formulated equations. The dimensions of the Quaife components that are used in these plots are shown below. The preload torque values for these comparisons come from the data collected for each experiment.

Table 3.3: Dimensions of the Quaife Components used in the Model Equations

DIMENSIONS		
PLANETARY GEAR		
Pitch Radius	0.285	in
Pressure Angle	20	deg
Helix Angle	23	deg
SUN GEAR		
Pitch Radius	0.8705	in
Pressure Angle	20	deg
Helix Angle	23	deg
CASE		
Planetary Pocket Radius	1.225	in
Coefficent of Friction	0.21	
END PLATE		
Coefficient of Friction	0.21	
SPROCKET		
Pitch Radius	4.48	in

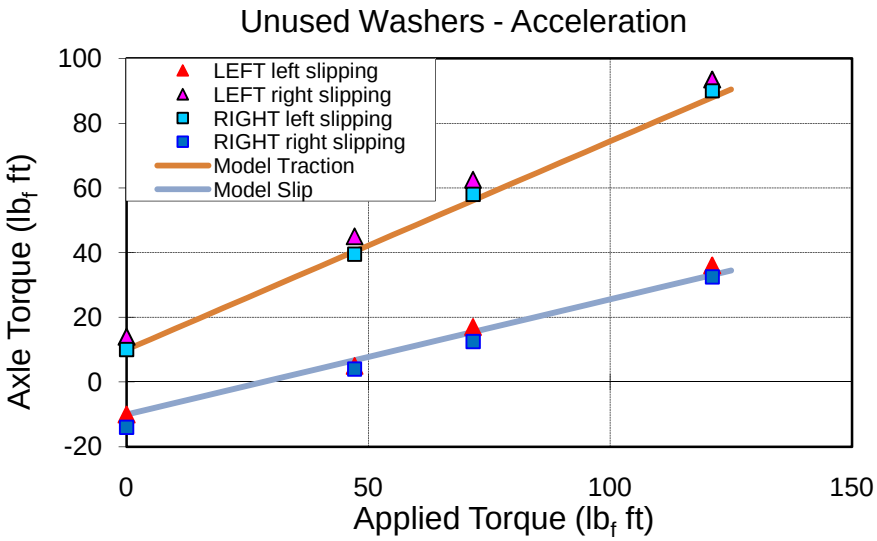

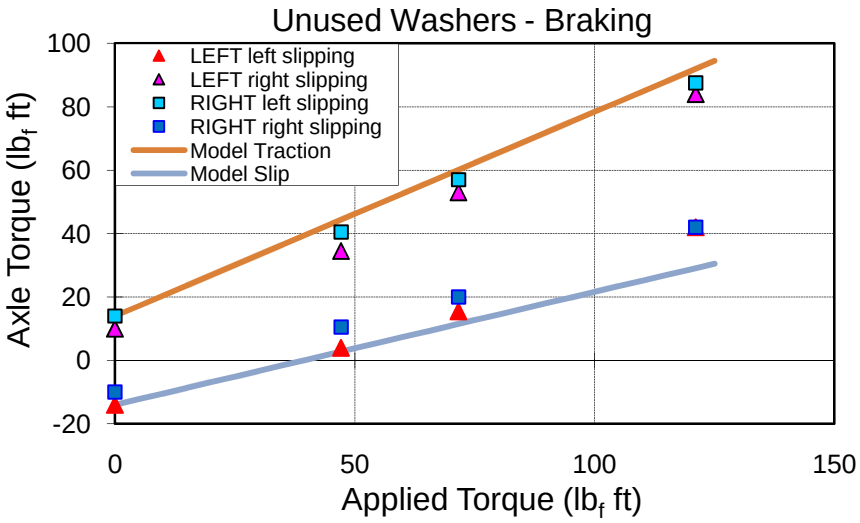

Figure 3.14: Model verses Stock Configuration using Unused Washers

Figure 3.14 shows the comparison between the test results for the stock configuration using unused Bellville washers and to plots taken from the equations. For this test the acceleration preload is +/- 10 foot-pounds of torque, and the braking preload is +/- 14 foot-pounds of torque.

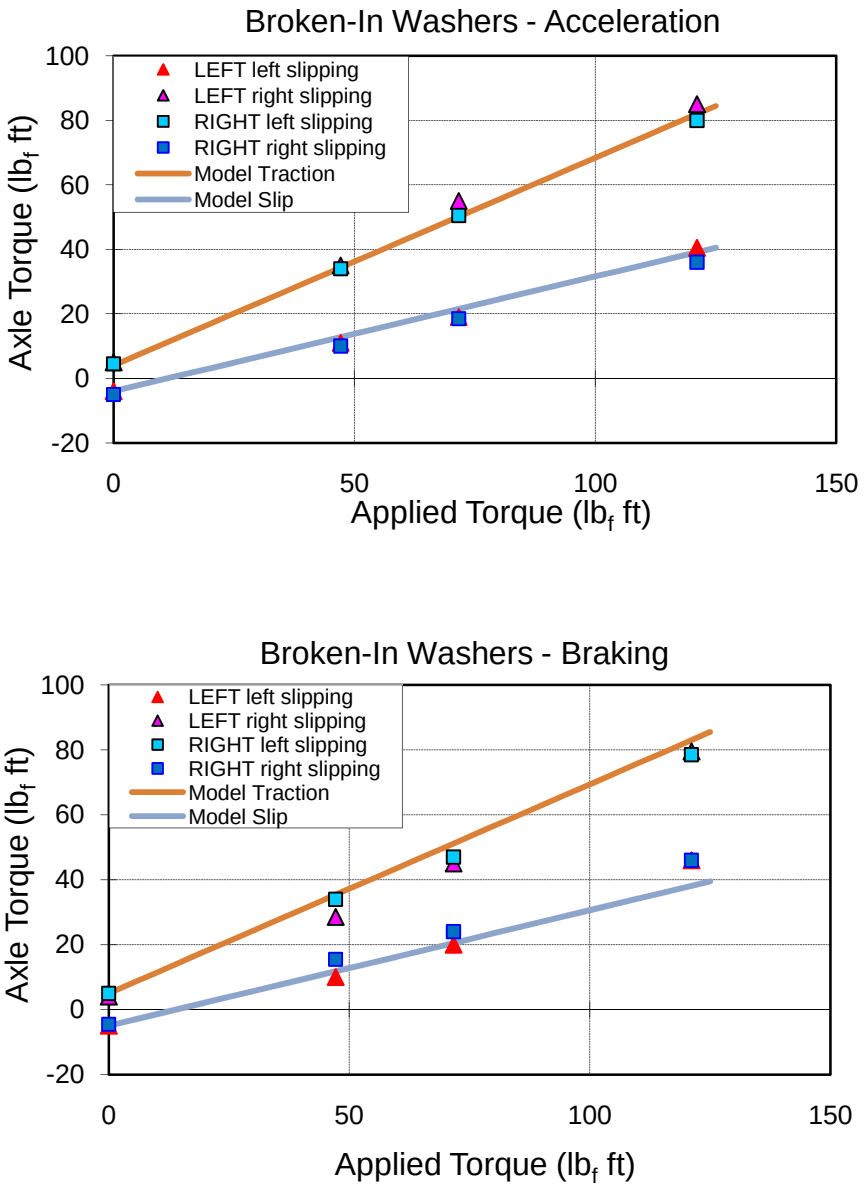

Figure 3.15: Model verses Stock Configuration using Broken-In Washers

Figure 3.15 compares the stock configuration with broken-in Bellville washers to the model. The acceleration preload is +/- 4 foot-pounds of torque, and the braking preload is +/- 5 foot-pounds of torque.

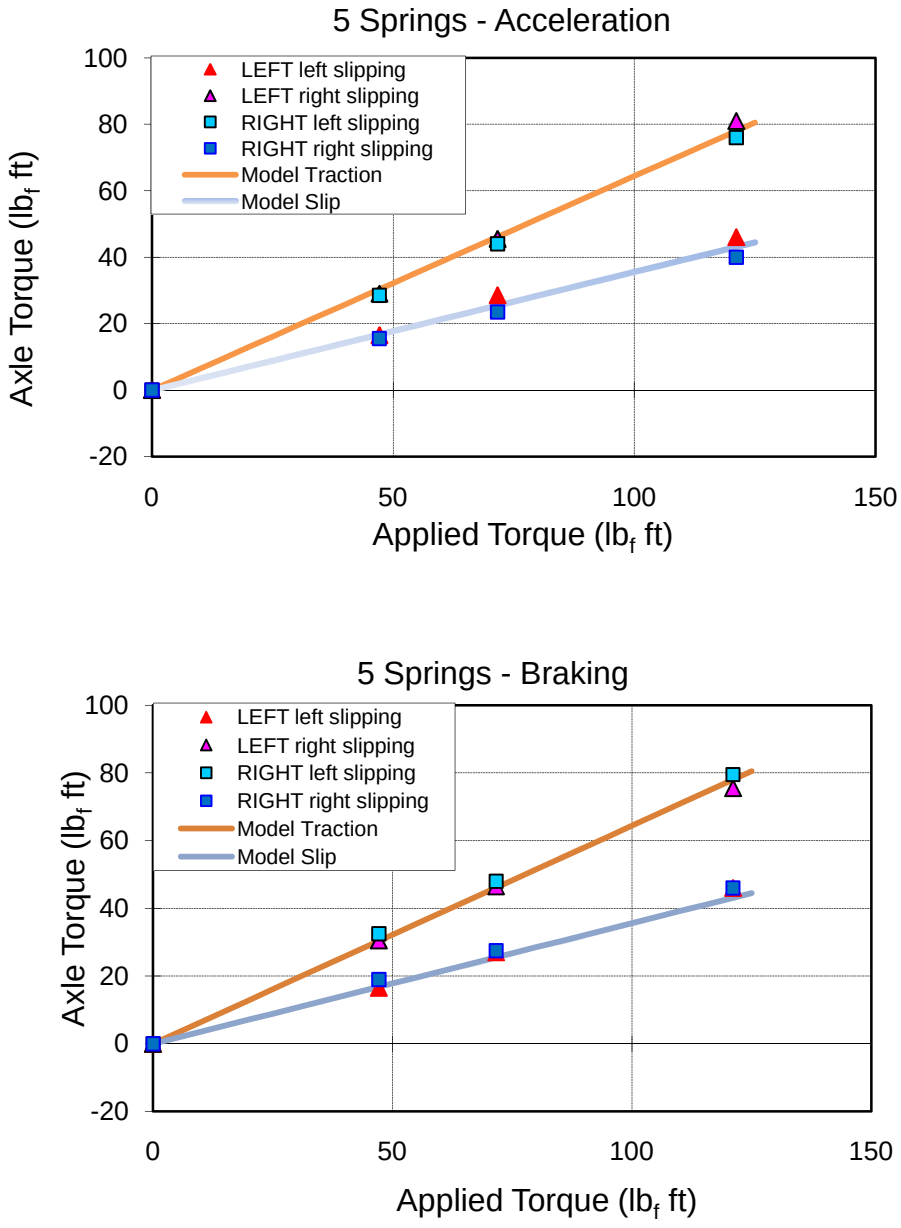

Figure 3.16: Model verses Five Washer Configuration

Figure 3.16 compares the test using only five Bellville washers to the model. There is 0 foot-pounds of preload torque.

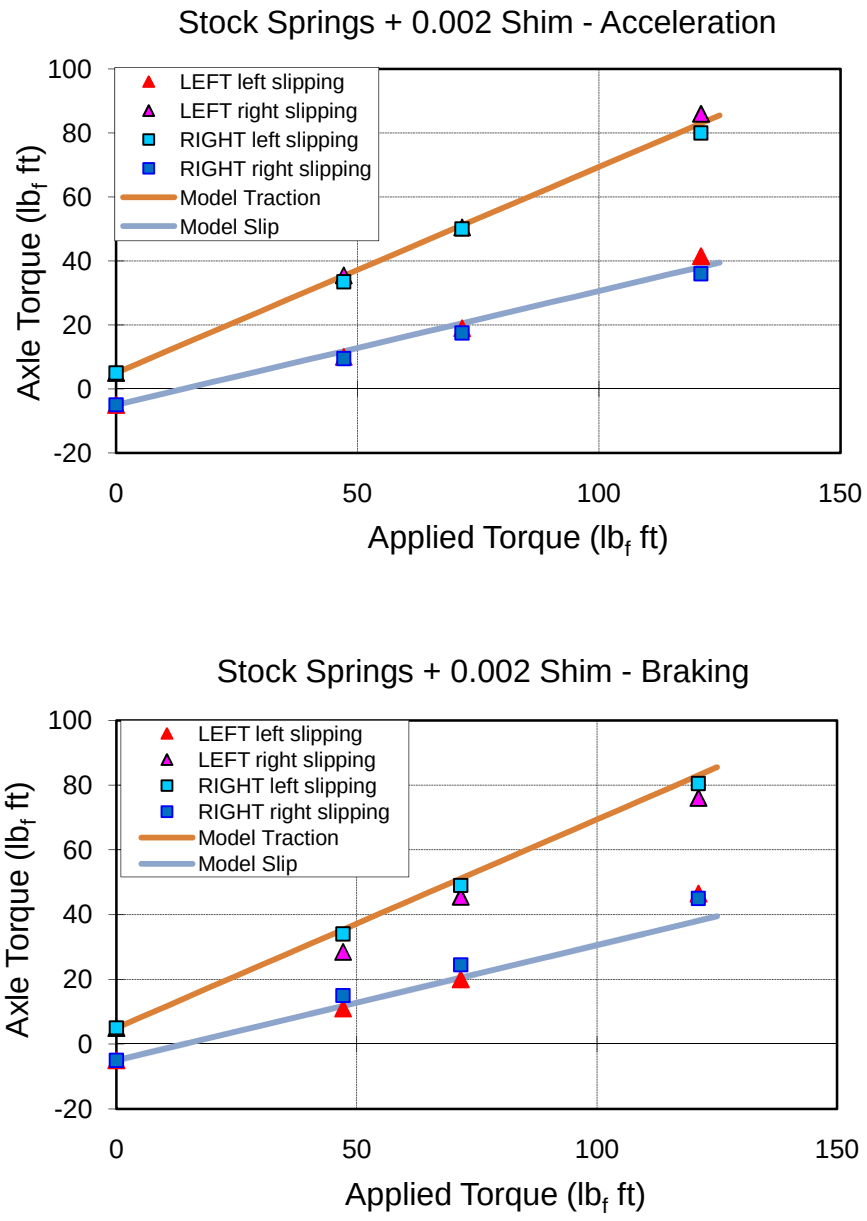

Figure 3.17: Model verses Stock Plus 0.002 Inch Shim

Figure 3.17 compares the stock configuration with a 0.002 inch shim to the model. For this comparison both the acceleration and braking preload is +/- 5 foot-pounds of torque.

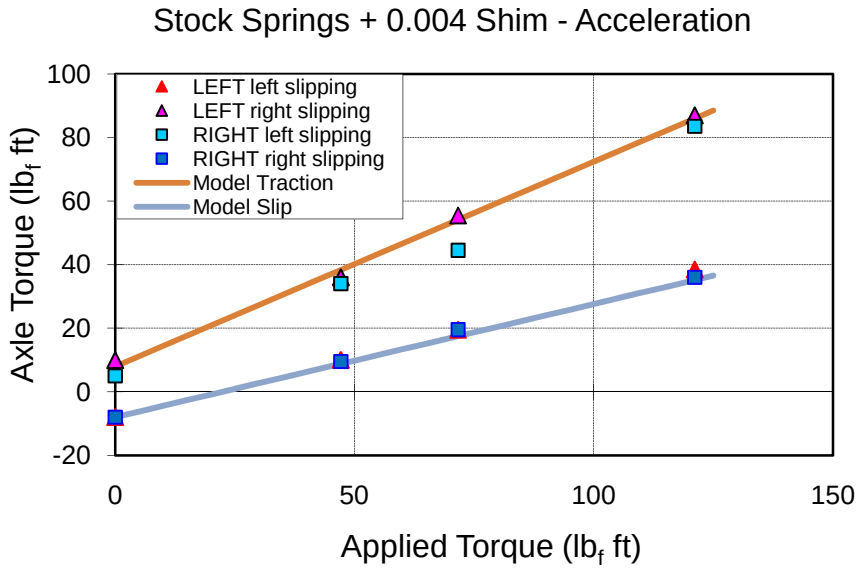

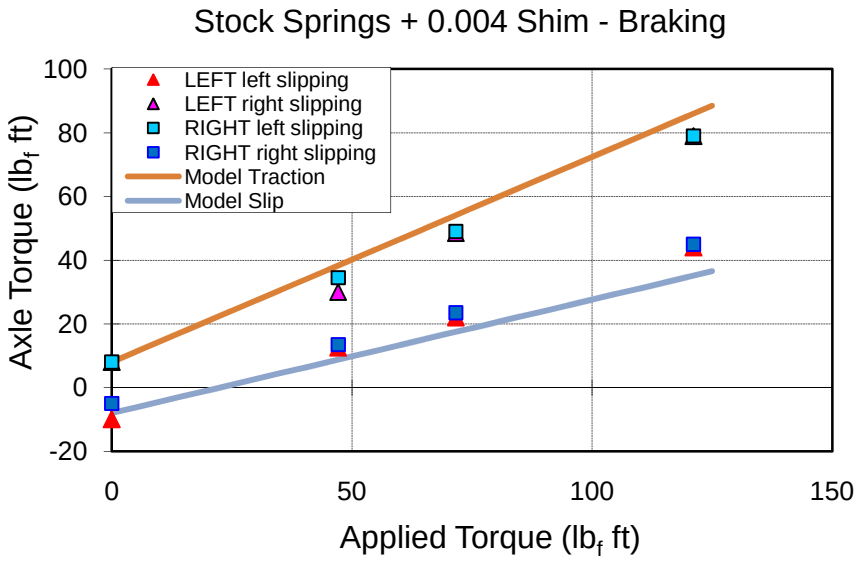

Figure 3.18: Model verses Stock Plus 0.004 Inch Shim

Figure 3.18 compares the stock configuration with a 0.004 inch shim to the model. For this comparison both the acceleration and braking preload is +/- 8 foot-pounds of torque.

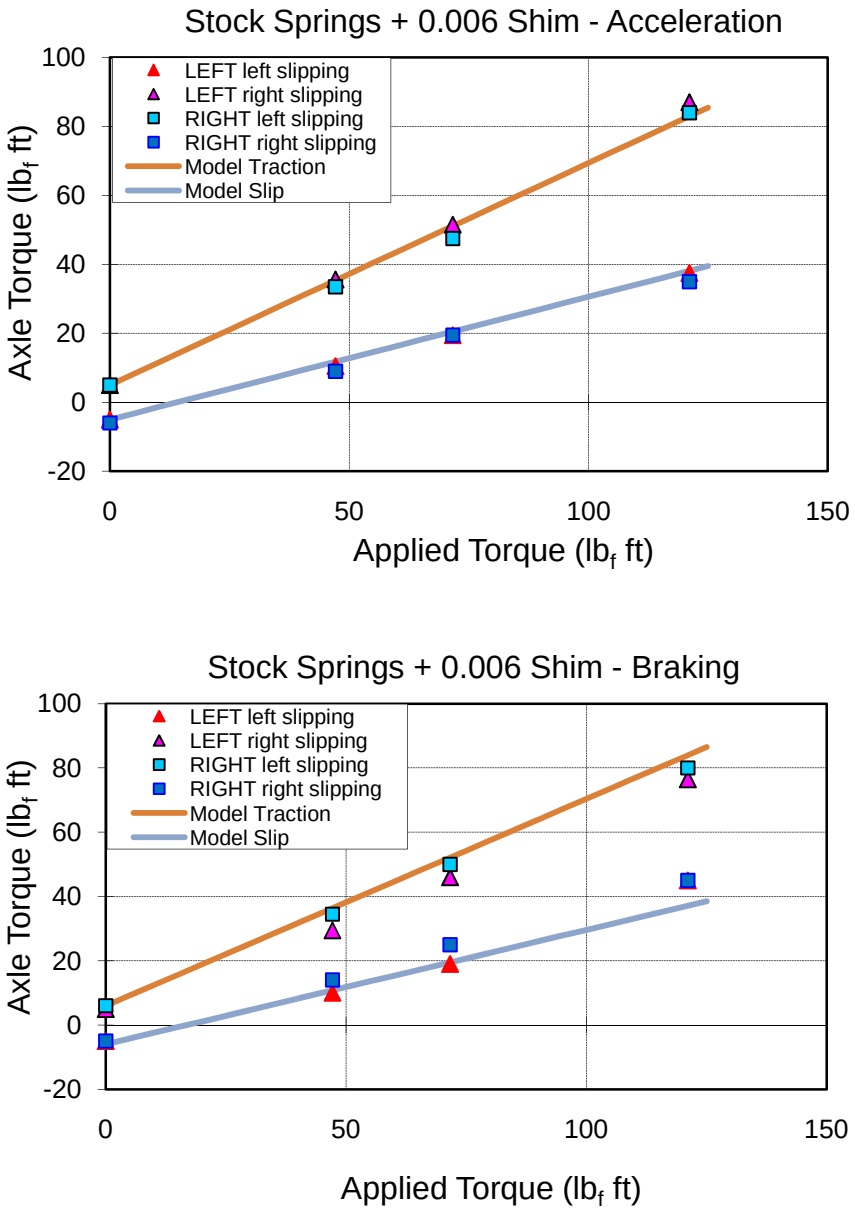

Figure 3.19: Model verses Stock Plus 0.006 Inch Shim

Figure 3.19 compares the stock configuration with a 0.006 inch shim to the model. The acceleration preload is +/- 5 foot-pounds of torque, and the braking preload is +/- 6 foot-pounds of torque.

It can be seen from the comparisons that test results follow the plots generated from Equations (6) and (7). Tables 3.4 and 3.5 summarize the comparison between the model and the experimental data.

Table 3.4: Acceleration Bias Ratios Found from the Test Results

	126.3 lb_f Load			191.9 lb_f Load			324.4 lb_f Load		
		Test, %			Test, %			Test, %	
Configuration	Model, %	Left Slip	Right Slip	Model, %	Left Slip	Right Slip	Model, %	Left Slip	Right Slip
Unused Washers	86	84	95	78	81	87	76	74	77
Broken-In Washers	73	72	74	70	70	77	68	66	70
5 Washers	64	60	62	64	61	64	65	63	67
0.002 Shim	75	71	75	71	70	70	69	66	71
0.004 Shim	81	72	76	75	62	77	71	69	72
0.006 Shim	75	71	76	71	66	72	71	69	72

Table 3.5: Braking Bias Ratios Found from the Test Results

	126.3 lb_f Load			191.9 lb_f Load			324.4 lb_f Load		
		Test, %			Test, %			Test, %	
Configuration	Model, %	Left Slip	Right Slip	Model, %	Left Slip	Right Slip	Model, %	Left Slip	Right Slip
Unused Washers	94	86	73	83	80	74	71	72	69
Broken-In Washers	75	72	60	71	66	63	66	65	66
5 Washers	64	69	65	64	67	65	64	66	62
0.002 Shim	75	72	60	71	68	64	65	66	63
0.004 Shim	81	73	64	75	68	68	65	65	65
0.006 Shim	77	73	63	72	70	64	65	66	63

Using these tables, Figures 3.20 and 3.21 were generated to show how the bias ratios correspond between the test results and the model.

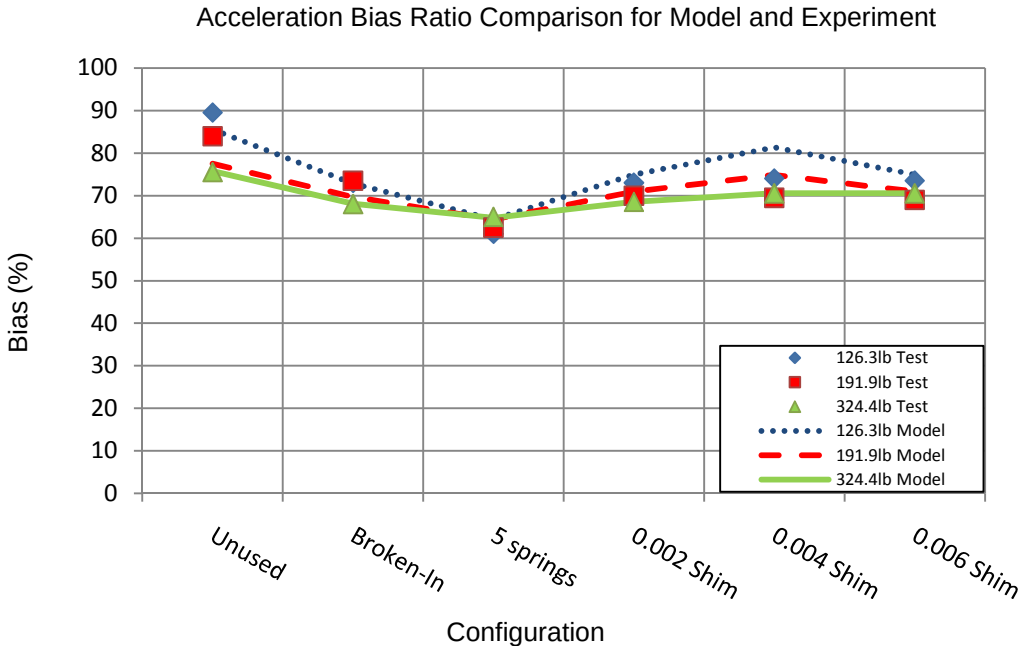

Figure 3.20: Acceleration Bias Ratio Comparison

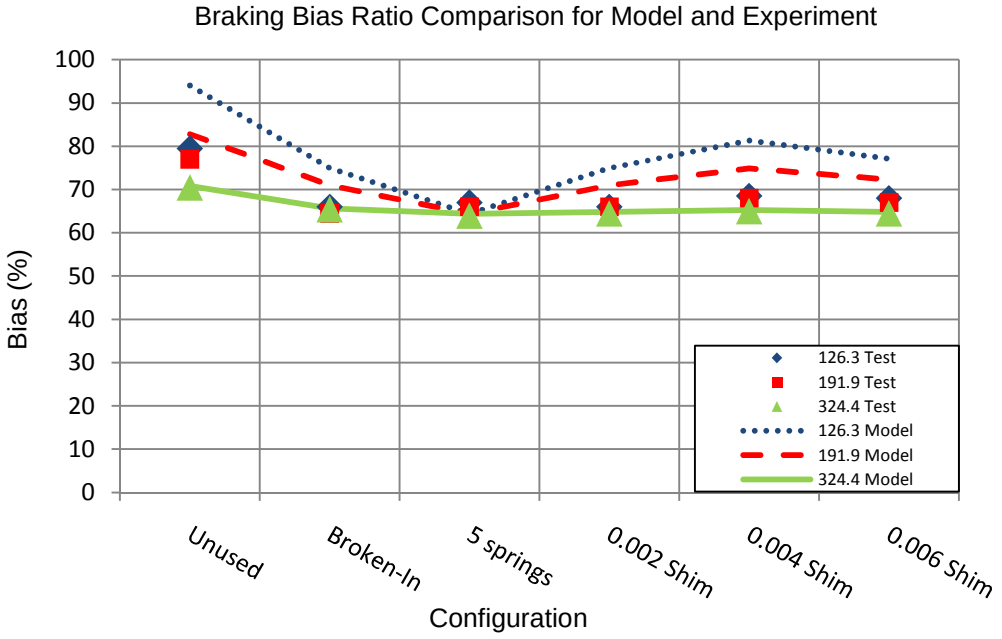

Figure 3.21: Braking Bias Ratio Comparison

It can be seen that the bias ratio of the model corresponds to the test data more accurately for the experiment using larger loads. This is due to the system having less mechanical backlash since the larger applied torque takes up the tolerances in the system. The highest bias ratio occurs when the Bellville washers are unused, while the lowest bias ratio occurs when only five Bellville washers are used. Also, it can be seen that both the model and test data follow the same trends.

CHAPTER 4

RECOMMENDATION

The experimental results show how the bias ratio can change due to a modification in the spring pack. From the formulated equation the coefficient of friction is the other variable that could be the most significant parameter to change. It is seen from Figure 17 that by increasing the coefficient of friction the traction and slip slopes will become steeper and the bias ratio will increase.

The coefficient of friction can be modified in several ways. One option is to use different viscosity gear oil. Scott Young at Taylor Race Engineering recommended 10M gear oil in lieu of the 75W90 gear oil that is commonly used. He has been working with other Formula SAE teams that have been experiencing inside tire spin during cornering which suggests either the coefficient of friction is too low with performance similar to an open differential or too high with performance similar to a locked differential. The 'M' in '10M' stands for 1000 centistokes; one centistoke is the viscosity of water (*Dynamic, Absolute and Kinematic Viscosity*, 2011). Through on-the-car testing, this gear oil has been found to eliminate inside wheel spin without any other changes to the differential. Other gear oils that Taylor Race Engineering has tested include 5M, 12M, 30M, and 60M. The coefficient of friction can also be modified by using materials other than steel for the case and the end plates. Taylor Race has developed an aluminum case that can replace the steel case, and the end plates could be replaced with a machined end plate of an alternative material. Another option is to insert a friction material between the interface of the end plates and the sun and planetary gears. Figure 4.1 is a model of how this could be accomplished.

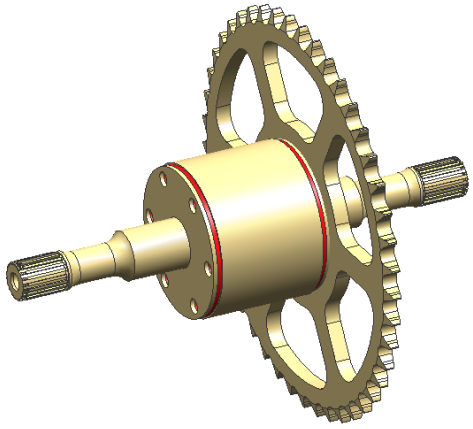

Figure 4.1: Quaife Model Modified with Additional Friction Plates

Plates could be made from a friction material and could sandwich between the case and the end plates. This is represented by the red parts in Figure 4.1. The coefficient of friction would be varied by choosing available materials whose friction constant is known.

CHAPTER 5

CONCLUSION

This thesis investigated the operation of the Quaife differential, modeled its mathematics, and determined how the preload torque affects its biasing ratio. The equations that were derived describe the behavior of the differential in terms of the preload torque and the coefficient of friction. It is recommended to have a high bias ratio to allow the most torque to transfer to the tire that has the most traction. The parameter that was modified for this investigation, the preload, was found to have an influence on the system but through further analysis it was determined that the bias ratio is more sensitive to the coefficient of friction. Recommendations were then made to show how the Quaife differential could be modified to test different coefficients of friction.

This investigation into the Quaife differential generated a new question: how will modifying the coefficient of friction affect the differentials torque biasing characteristics? To do this the differential could be modified using the method described in the Recommendations section, it could be tested using different gear oils, or the components could be machined from different materials.

APPENDIX A

EXPERIMENTAL DATA

UNUSED WASHERS

Date: 5-Jan-11

Trout & Woods

Friction Measurements

Acceleration Torque (lbf ft)		
Diff	**Left**	**Right**
0	-10	10
15	15	Diff Locked
15	Diff Locked	15

Braking Torque (lbf ft)		
Diff	**Left**	**Right**
0	14	-14
15	-15	Diff Locked
10	Diff Locked	-10

ACCELERATION

Left Slipping Torque (lbf ft)

Applied (lbf ft)	Left (lbf ft)	Right (lbf ft)	Total (lbf ft)	Bias (%)
0.0	-10	10	0	
47.2	5	39.5	44.5	84
71.6	17	58	75	81
121.1	36	90	126	74

Right Slipping Torque (lbf ft)

Applied (lbf ft)	Left (lbf ft)	Right (lbf ft)	Total (lbf ft)	Bias (%)
0.0	14	-14	0	
47.2	45	4	49	95
71.6	62.5	12.5	75	87
121.1	93.5	32.5	126	77

BRAKING

Left Slipping Torque (lbf ft)

Applied (lbf ft)	Left (lbf ft)	Right (lbf ft)	Total (lbf ft)	Bias (%)
0.0	-14	14	0	
47.2	4	40.5	44.5	86
71.6	15.5	57	72.5	80
121.1	42	87.5	129.5	72

Right Slipping Torque (lbf ft)

Applied (lbf ft)	Left (lbf ft)	Right (lbf ft)	Total (lbf ft)	Bias (%)
0.0	10	-10	0	
47.2	34.5	10.5	45	73
71.6	53	20	73	74
121.1	84	42	126	69

BROKEN-IN WASHERS

Date: 22-Feb-11

Trout & Woods

Friction Measurements

Acceleration Torque (lbf ft)		
Diff	**Left**	**Right**
0	-4	4.5
13	13	Diff Locked
10	Diff Locked	10

Braking Torque (lbf ft)		
Diff	**Left**	**Right**
0	5	-5
19	-19	Diff Locked
13	Diff Locked	-13

ACCELERATION

Left Slipping Torque (lbf ft)

Applied (lbf ft)	Left (lbf ft)	Right (lbf ft)	Total (lbf ft)	Bias (%)
0.0	-4	4.5	0.5	
47.2	11	34	45	72
71.6	19	51	69.5	70
121.1	41	80	120.5	66

Right Slipping Torque (lbf ft)

Applied (lbf ft)	Left (lbf ft)	Right (lbf ft)	Total (lbf ft)	Bias (%)
0.0	5	-5	0	
47.2	35	10	45	74
71.6	55	19	73.5	77
121.1	85	36	121	70

BRAKING

Left Slipping Torque (lbf ft)

Applied (lbf ft)	Left (lbf ft)	Right (lbf ft)	Total (lbf ft)	Bias (%)
0.0	-5	5	0	
47.2	10	34	44	72
71.6	20	47	67	66
121.1	46	79	124.5	65

Right Slipping Torque (lbf ft)

Applied (lbf ft)	Left (lbf ft)	Right (lbf ft)	Total (lbf ft)	Bias (%)
0.0	4	-4.5	-0.5	
47.2	29	16	44	60
71.6	45	24	69	63
121.1	80	46	125.5	66

5 WASHER STACKUP TEST

Date: 12-Feb-11

Trout & Woods

Friction Measurements

Acceleration Torque (lbf ft)		
Diff	Left	Right
0	0	0

Braking Torque (lbf ft)		
Diff	Left	Right
0	0	0

ACCELERATION

	Left Slipping Torque (lbf ft)					Right Slipping Torque (lbf ft)				
Applied (lbf ft)	Left (lbf ft)	Right (lbf ft)	Total (lbf ft)	Bias (%)		Applied (lbf ft)	Left (lbf ft)	Right (lbf ft)	Total (lbf ft)	Bias (%)
0.0	0	0	0			0.0	0	0	0	
47.2	17	29	45	60		47.2	29	16	44.5	62
71.6	29	44	72.5	61		71.6	46	24	69	64
121.1	46	76	122	63		121.1	81	40	121	67

BRAKING

	Left Slipping Torque (lbf ft)					Right Slipping Torque (lbf ft)				
Applied (lbf ft)	Left (lbf ft)	Right (lbf ft)	Total (lbf ft)	Bias (%)		Applied (lbf ft)	Left (lbf ft)	Right (lbf ft)	Total (lbf ft)	Bias (%)
0.0	0	0	0			0.0	0	0	0	
47.2	17	33	49	69		47.2	31	19	49.5	65
71.6	27	48	75	67		71.6	47	28	74	65
121.1	46	80	125.5	66		121.1	76	46	121.5	62

STOCK WASHER STACKUP + .002 SHIM TEST

Date: 12-Feb-11

Trout & Woods

Friction Measurements

Acceleration Torque (lbf ft)		
Diff	**Left**	**Right**
0	-5	5
15	15	Diff Locked
15	Diff Locked	15

Braking Torque (lbf ft)		
Diff	**Left**	**Right**
0	5	-5
15	-15	Diff Locked
10	Diff Locked	-10

ACCELERATION

Left Slipping Torque (lbf ft)

Applied (lbf ft)	Left (lbf ft)	Right (lbf ft)	Total (lbf ft)	Bias (%)
0.0	-5	5	0	
47.2	10	34	43.5	71
71.6	19	50	69	70
121.1	42	80	121.5	66

Right Slipping Torque (lbf ft)

Applied (lbf ft)	Left (lbf ft)	Right (lbf ft)	Total (lbf ft)	Bias (%)
0.0	5	-5	0	
47.2	36	10	45	75
71.6	51	18	68	70
121.1	86	36	122	71

BRAKING

Left Slipping Torque (lbf ft)

Applied (lbf ft)	Left (lbf ft)	Right (lbf ft)	Total (lbf ft)	Bias (%)
0.0	-5	5	0	
47.2	11	34	45	72
71.6	20	49	69	68
121.1	47	81	127	66

Right Slipping Torque (lbf ft)

Applied (lbf ft)	Left (lbf ft)	Right (lbf ft)	Total (lbf ft)	Bias (%)
0.0	5	-5	0	
47.2	29	15	43.5	60
71.6	46	25	70	64
121.1	76	45	121	63

STOCK WASHER STACKUP + .004 SHIM TEST

Date: 12-Feb-11

Trout & Aaron

Friction Measurements

Acceleration Torque (lbf ft)		
Diff	**Left**	**Right**
0	-8	5
15	15	Diff Locked
12	Diff Locked	12

Braking Torque (lbf ft)		
Diff	**Left**	**Right**
0	10	-8
20	-20	Diff Locked
15	Diff Locked	-15

ACCELERATION

	Left Slipping Torque (lbf ft)			
Applied (lbf ft)	**Left (lbf ft)**	**Right (lbf ft)**	**Total (lbf ft)**	**Bias (%)**
0.0	-8	5	-3	
47.2	10	34	44	72
71.6	20	45	64	62
121.1	39	84	122	69

	Right Slipping Torque (lbf ft)			
Applied (lbf ft)	**Left (lbf ft)**	**Right (lbf ft)**	**Total (lbf ft)**	**Bias (%)**
0.0	10	-8	2	
47.2	36	10	45.5	76
71.6	56	20	75	77
121.1	87	36	123	72

BRAKING

	Left Slipping Torque (lbf ft)			
Applied (lbf ft)	**Left (lbf ft)**	**Right (lbf ft)**	**Total (lbf ft)**	**Bias (%)**
0.0	-10	8	-2	
47.2	13	35	47	73
71.6	22	49	71	68
121.1	44	79	123	65

	Right Slipping Torque (lbf ft)			
Applied (lbf ft)	**Left (lbf ft)**	**Right (lbf ft)**	**Total (lbf ft)**	**Bias (%)**
0.0	8	-5	3	
47.2	30	14	43.5	64
71.6	49	24	72	68
121.1	79	45	124	65

STOCK WASHER STACKUP + .006 SHIM TEST

Date: 12-Feb-11

Trout & Woods

Friction Measurements

Acceleration Torque (lbf ft)		
Diff	**Left**	**Right**
0	-5	5
17	17	Diff Locked
15	Diff Locked	15

Braking Torque (lbf ft)		
Diff	**Left**	**Right**
0	5	-6
21	-21	Diff Locked
12	Diff Locked	12

ACCELERATION

Left Slipping Torque (lbf ft)

Applied (lbf ft)	Left (lbf ft)	Right (lbf ft)	Total (lbf ft)	Bias (%)
0.0	-5	5	0	
47.2	11	34	44	71
71.6	20	48	67	66
121.1	38	84	121.5	69

Right Slipping Torque (lbf ft)

Applied (lbf ft)	Left (lbf ft)	Right (lbf ft)	Total (lbf ft)	Bias (%)
0.0	5	-6	-1	
47.2	36	9	44.6	76
71.6	52	20	71	72
121.1	87	35	122	72

BRAKING

Left Slipping Torque (lbf ft)

Applied (lbf ft)	Left (lbf ft)	Right (lbf ft)	Total (lbf ft)	Bias (%)
0.0	-5	6	1	
47.2	10	35	44.5	73
71.6	19	50	69	70
121.1	45	80	125	66

Right Slipping Torque (lbf ft)

Applied (lbf ft)	Left (lbf ft)	Right (lbf ft)	Total (lbf ft)	Bias (%)
0.0	5	-5	0	
47.2	30	14	43.5	63
71.6	46	25	71	64
121.1	77	45	121.5	63

REFERENCES

1. *Friction and Coefficients of Friction* (2011, March 4). The Engineering Toolbox. Retrieved March 12, 2011 from http://www.engineeringtoolbox.com/friction-coefficients-d_778.html.
2. *Dynamic, Absolute and Kinematic Viscosity* (2011, March 12). Retrieved March 12, 2011 from http://www.engineeringtoolbox.com/dynamic-absolute-kinematic-viscosity-d_412.html.
3. Mott, Robert L. (2004). *Machine Elements in Mechanical Design* (4th Ed.). Upper Saddle River: New Jersey, Pearson Education, Inc.
4. Scott Young (Technical Advisor at Taylor Race Engineering) [Email and Interview at Taylor Race Engineering on January 18, 2011]
5. Chocholek, S.E. (1988). The development of a differential for the improvement of traction control [Electronic Version]. C368/88 © IMechE 1988.
6. *Static & Kinetic Friction* (2011, March 21). *David Newman's Page*. Web. 21 Mar. 2011. http://ffden-2.phys.uaf.edu/211_fall2002.web.dir/ben_townsend/staticandkineticfriction.htm.
7. *Quaife Differentials* (2011, March 28). Web. <http://www.quaife-differentials.com/>.

BIOGRAPHICAL INFORMATION

John W. H. Trout graduated with a Bachelor of Science in Mechanical Engineering from Texas A&M University in 2006. He has been involved with the Formula SAE program at the University of Texas in San Antonio as well as at Texas A&M University where he worked on the drive train team to help win Formula SAE West of 2006. He has been working at Bell Helicopter since the summer of 2006 in the areas of wiring, controls, hydraulic, furnishings, and equipment. His interests include automotive engineering, thermodynamics, controls, and alternative energy.